Norwegian University
of Life Sciences

Master's Thesis 2018 60 ECTS

Faculty of Environmental Sciences and Natural Resource Management
Kari Klanderud
Pernille B. Eidesen, UNIS
Inger G. Alsos, UiT

The Holocene vegetation history of an isolated, high-arctic plant diversity hot spot

Linn Margrethe Høeg Voldstad
Master of Science in Ecology

Acknowledgements

This study comprises data from many different scientific fields and proved to demand experience and knowledge quite far beyond my prior experience. I owe many thanks to everyone who helped me and made this study possible: Wesley Farnsworth (The University centre in Svalbard) and Anders Schomacker (The Arctic University of Norway) for access to the sub-samples of the sediment cores and all core-related data (project 16/35 funded by the Carlsberg Foundation). The ECOGEN research group in Tromsø, and in particular Youri Lammers, Peter Heintzman and Dilli Rijal for help with bioinformatics (Youri), guidance in the aDNA lab (Peter) and for running the metabarcoding PCRs and pooling and cleaning the PCR products (Peter and Dilli). Johannes Sand Bolstad for assisting with field work. Lena Håkansson (The University Centre in Svalbard) for guidance and help with interpreting geological data. Jan Christensen's endowment for financial support. Special thanks go to all my supervisors, and in particular Pernille B. Eidesen for giving me the opportunity to explore the flora in Ringhorndalen, and in general for her enthusiasm and advice during the whole process.

Abstract

Through high throughput sequencing of ancient, environmental DNA collected from lake sediment cores (*sed*aDNA), this study revealed postglacial vegetation change during the last ~12.000 years in a high-Arctic plant diversity hot spot in Svalbard. Geochemical proxy data for environmental variation in the catchment area obtained from high resolution X-radiographic scans were combined with the *sed*aDNA record to detect local Holocene climate variations. The findings were in accordance with main climatic shifts on Svalbard identified by previous studies and indicated an early warm and species-rich postglacial period followed by fluctuating cool and warming events throughout the Holocene record. Thermophilic species with their current distribution outside the catchment area of the studied lake had reoccurring presence throughout the Holocene *sed*aDNA record, suggesting postglacial periods when thermophilic arctic species had broader distribution ranges than today. This supports the hypothesis of isolated relict populations in Ringhorndalen, the place in Svalbard with the highest registered diversity of vascular plants and several remarkable and isolated plant populations located far north of their normal distribution range.

Introduction

Paleoecological records provide insight into past vegetation. This information can be combined with knowledge about past climates in order to anticipate impacts from global warming on species diversity and composition in an area (Allen & Huntley 1999). Knowledge about the historic plant species composition can even be used to increase knowledge about past climates (Alsos et al. 2015). Next generation sequencing methods have drastically increased the potential for molecular investigations in paleoecological studies in the last decade (Taberlet et al. 2007; Parducci et al. 2017). In particular have ancient DNA from sediments (*sed*aDNA) shown to be an efficient tool for reconstructing past vegetation and species diversity in environments where more traditional paleobotanical methods can be challenging due to low pollen and plant macrofossil concentrations (Taberlet et al. 2007; Sønstebø et al. 2010; Jørgensen et al. 2012; Pedersen et al. 2013; Alsos et al. 2015; Parducci et al. 2017).

Ancient DNA studies can be particularly useful to reconstruct past vegetation in the arctic regions, because low local pollen concentrations impede traditional methods (Vasil'chuk 2005) and the cold conditions ensure preservation of the genetic material (Hofreiter et al. 2001). Even if DNA is highly degraded, which is increasingly likely with older sample material (Hofreiter et al. 2001), studies from arctic regions have proven the value of modern sequencing technologies when analysing DNA directly from environmental samples, such as sediments (Sønstebø et al. 2010).

Preservation and recovery of *sed*aDNA is particularly good in lake sediments (Parducci et al. 2017; Alsos et al. 2018). Lake sediments also hold information about regional climate change because they trap detrital and organic material as well as organic material produced within the lake (Gjerde et al. 2017). Magnetic and geochemical properties obtained from high-resolution X-radiographic scans can be used as proxies to study major patterns in abiotic environmental changes in the catchment area of the studied lake. The variation in scanned profiles of magnetic susceptibility and lithogenic, geochemically stable and conservative elements such as aluminium (Al), silica (Si), potassium (K), titanium (Ti), iron (Fe) and rubidium (Rb) can reflect changes in glacial-derived minerogenic input (Sandgren & Snowball 2001), weathering regimes (Rothwell & Croudace 2015) or the amount of inorganic detrital input to a lake (Røthe et al. 2015), thus be used to infer climate variations. The elements calsium (Ca) and silica (Si) normalized against Ti and and iron (Fe) normalized against manganese (Mn) can be used as proxies for biological productivity within the lake (Balascio et al. 2011; Kylander et al. 2011;

Melles et al. 2012; Alsos et al. 2015; Gjerde et al. 2017).

*Sed*aDNA and plant macrofossil records from lakes in western Spitsbergen have shown that thermophilic plant species probably had a broader distribution on Spitsbergen in early Holocene, a warmer postglacial period (Birks 1991; Alsos et al. 2015). An area that assumingly has remains from this vegetation, is Ringhorndalen (Eidesen et al. 2013). This tributary valley east of Wijdefjorden, Spitsbergen, have been described as an 'Arctic hotspot' as defined by Elvebakk (2005a), with numerous registrations of thermophilous species. One remarkable botanical feature of Ringhorndalen is that many of the unusual plant species observed there seem to be spatially distant from their normal distribution range. Some populations represent some of the northernmost known sites for the species worldwide and in some cases the only known location for Svalbard and even Europe (Eidesen et al., unpublished).

In this study I investigated a *c.* 12 000-year-old sediment core from a high-arctic lake in Ringhorndalen using *sed*aDNA, sediment properties and geochemical proxy data, in order to reconstruct changes in vegetation composition and evaluate these changes in a context of a changing Holocene climate. It is assumed that the postglacial period *c*. 9000-5000 years ago was remarkably warmer than present (Hyvärinen 1970; Birks 1991; Birks et al. 1994; Salvigsen & Høgvard 2006; Miller et al. 2010; Alsos et al. 2015; Mangerud & Svendsen 2018), thus vegetation reconstructions from this period can provide information about possible future vegetation development in scenarios with anticipated warming in the Arctic.

The research questions I aimed to answer were: (i) How has the composition of plants in the catchment area of the studied high-arctic lake developed during the Holocene? (ii) How does the variation in climatic conditions revealed from biotic and abiotic sources match throughout the depth of the core? (iii) How is the current vegetation around the lake represented in the modern, uppermost sediment layers? (iv) Are the unusually thermophilic vascular plant species found in Ringhorndalen today relicts from populations established during the Holocene warm periods?

To address these research questions, historic postglacial plant species assemblages were obtained from amplicon high-throughput sequencing (HTS) of *sed*aDNA sampled chronologically throughout the core. Obtained vegetation data were compared to geochemical data acquired through high-resolution X-radiographic scans (Croudace et al. 2006). Plant species assemblages representing the current vegetation were obtained from HTS of DNA in

the uppermost sediment layer. The current vegetation data from modern sediments were then compared to the present floristic composition acquired from on-site vegetation analysis. Results from the *sed*aDNA analysis were also used to investigate the origin of unusually thermophilic species registered in Ringhorndalen. Species that matched between ancient and present plant assemblages were assumed to represent long-time presence, and to disclose these populations as remnants from a former more widespread vegetation from the warmer early Holocene (Eidesen et al. 2013). Alternatively, these isolated populations can be recent colonizers, and must be seen in context with ongoing climate change. In the latter case, the findings of this study represent an important contribution to the understanding of species immigration to Svalbard. As Ringhorndalen is rarely visited by people, any recent plant establishments here are likely to be due to natural long-distance dispersal, as former studies have shown to frequently occur in Svalbard (Alsos et al. 2007).

Methods

Study area

Indre Wijdefjorden National Park was established in 2005 as a result of thorough botanical investigations that revealed remarkable findings at several locations in the area (Elvebakk & Nilsen 2002). These findings included populations of rare and unusually thermophilous plants in an arctic context. In addition, a new vegetation type was described – the high-arctic steppe (Elvebakk 2005b).

Ringhorndalen (79.32°N, 16.12°E) is situated at the northern border of Indre Wijdefjorden National Park (Fig. 1) but was not investigated as part of the initial survey in 2002 (Elvebakk & Nilsen). Later investigations of Ringhorndalen and the neighbouring valley Flatøyrdalen have revealed an unusually high biodiversity. A total of 124 registered vascular plant species makes this area the most botanically diverse location in Svalbard, with several species found exclusively in Ringhorndalen (Eidesen et al., unpublished).

Even though no climatic record exists for the area, the vegetation in the outer areas reflect relatively high temperatures combined with aridity due to little precipitation and wind desiccation, and limescale enrichments from marine sediment deposits up to ca. 80 m a. s. l. (Elvebakk & Nilsen 2002). Further in the valley of Ringhorndalen, there are areas sheltered from wind, and with additional supply of water. Two glacier arms extend down furthest into the valley from a large ice cap on the eastern side. The valley bottom is mostly covered by a

discontinuous meltwater river fed by glacier runoff, and surrounding floodplains and wetland. On the steep valley sides, particularly lush gulleys, open screes and sheltered boulder fields stretches down from cliffs higher up, whereas *Cassiope tetragona* heath dominates further down. The high-Arctic steppe, with prevalent *Potentilla pulchella* communities, is distinct in the entrance of the valley, close to the fjord, where the wind tunnel effect from Wijdefjorden is strongest. A few small ridges and lakes separate the outskirts from the warmer and more sheltered sites further into the valley. Temperature loggers placed in the south facing slope of Ringhorndalen from May to August 2017 recorded maximum temperatures of 42°C in the soil layer in vegetated cliffs (P. Eidesen, unpublished results). It is likely that the wide range of habitats combined with the unusual climatic conditions facilitates a diverse and unique vegetation that makes Ringhorndalen an interesting location to study vegetation history in Svalbard.

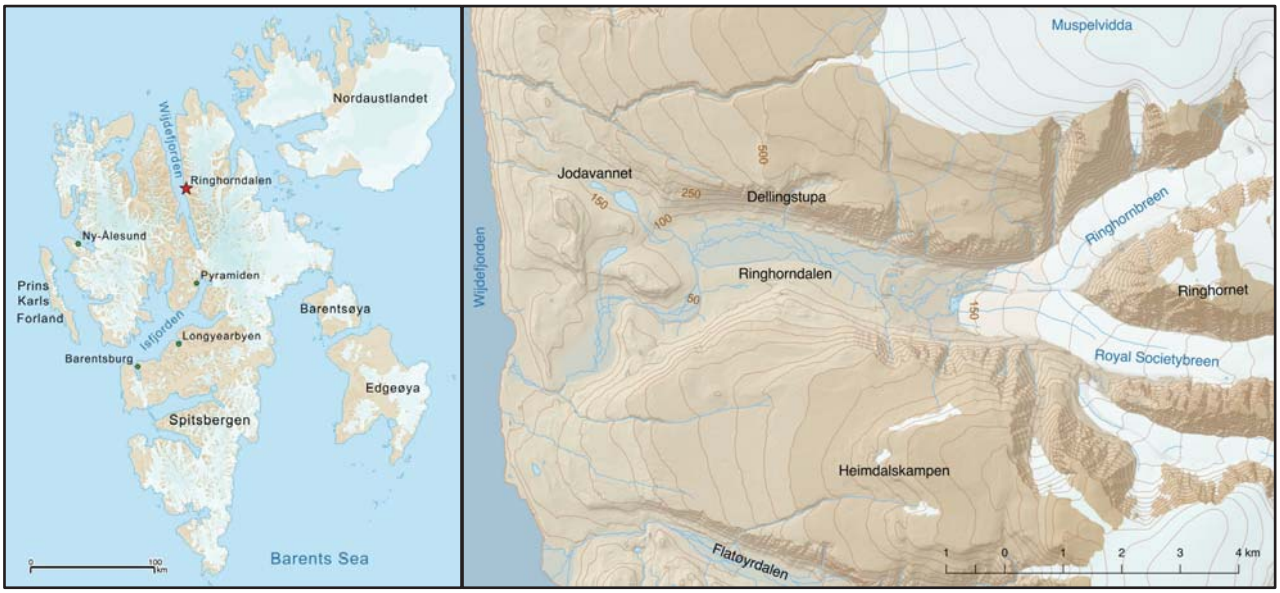

Figure 1: The archipelago of Svalbard (left frame), marking the study area Ringhorndalen (red star). Close up of study location (right frame). Maps modified (QGIS 2.18.15 2016) from Norwegian Polar Institute/USGS Landsat (2010), with overlaying details (lakes, rivers, glaciers, contours) from Norwegian Polar Institute (2014a) and underlaid with 5m digital elevation model (Norwegian Polar Institute 2014b).

The analysed sediment cores were obtained from a high-arctic lake hereafter called *Jodavannet* (79.3383°N, 16.0167°E; Fig. 1 and 2). Jodavannet is situated 140 m a. s. l. in the elevated areas on the northern side of the valley's entrance. It is regarded a *threshold lake*, meaning it has transitioned between being glacier-fed in times of relatively extensive ice cover, and receiving non-glacial, organic-rich sediments during times of relatively restricted ice cover (Briner et al.

2010; Schomacker et al. 2016). Jodavannet is currently non-glacial, as the catchment area does not receive input from glacier run-off due to topographic boundaries between the lake and the glaciers in close proximity (Fig. 1). The slopes on the northern, western and southern sides of the lake are slightly inclined towards the lake, causing inlet of water from the pass approximately 10 metres above the lake on the north-western side. Also, traces of erosion from water flow towards the lake can easily be seen on the southern and south-western side (Fig. 2). In the south-eastern end, there is an outlet leading to a lake about three times as big as Jodavannet (Fig. 1).

The vegetation around Jodavannet is relatively homogenous, with a moss-dominated belt stretching several metres (~5 m.) from the lake edge. Dominating vascular plant species in the closest 30 meters around the lake are *Saxifraga oppositifolia, Carex subspathacea, Dupontia fisheri, Bistorta vivipara, Salix polaris* and *Equisetum arvense* ssp. *alpestre*. *Cardamine pratensis* is relatively abundant within close proximity to the lake edge, while *Dryas octopetala* and *Cassiope tetragona* has scattered occurrences further away.

General remarks

This study comprised considerable amounts of data from many different sources. Such a composition of data was possible due to access to external data, meaning not all sampling described were conducted by me. Sampling and subsampling of the sediment core, geochemical analysis, radiocarbon dating, PCR amplification, purification and pooling of PCR-products and metabarcoding were conducted by others (specified in the relevant sections). The described methodologies were conducted by myself if nothing else is specified.

Sediment core and radiocarbon dating

The sediment cores were acquired by W. Farnsworth (The University Centre in Svalbard) and A. Schomacker (The Arctic University of Norway). One surface core and one piston core were retrieved from Jodavannet using lightweight manual corers during a field campaign in August 2016. The 68 cm long surface core was taken with a gravity corer (Farnsworth et al. 2016), while a hand-held piston corer with 60 mm diameter coring tubes was used for the 186 cm long piston core (Schomacker et al. 2016). The cores were sampled at approximately the same point (79.33831°N, 16.01902°E), with the surface core taken first as the piston corer tends to destroy the surface sediments. The cores had a slight offset between them, as the piston core lacked approximately the upper 10 cm that the surface core had. The cores were sealed, kept cold (3-

4°C) and closed until arrival at the Centre for GeoGenetics in Copenhagen, Denmark. Farnsworth and A. Rouillard (The University of Copenhagen) did the core opening, -splitting, and subsequent subsampling of sediments and macrofossils, following the sampling procedures developed by Pedersen et al. (2016). In order to extract *sed*aDNA from the cores, sediments were subsampled in 2 cm intervals along the entire core lengths. The samples were kept cold and transported to the University Museum in Tromsø, Norway, where they were stored frozen until further processing. One core-half was kept intact as a reference. To establish the chronology of the sediment cores, six and three macrofossils were retrieved from the piston and surface core, respectively (Table 1). One aquatic macrofossil was collected to constrain the age at the base of the piston core, otherwise the macrofossils were of terrestrial origin. All nine macrofossils were ^{14}C dated with accelerator mass spectrometry (AMS) in the Tandem Laboratory at Uppsala University, Sweden.

I constructed age-depth models with function *Bacon* of the Bayesian statistics program Bacon 2.2 (Blaauw & Christen 2011) and the calibration curve IntCal13 (Reimer et al. 2013). The program divided the cores into many vertical sections of equal thickness and estimated sedimentation times (years/cm) through millions of Markov Chain Monte Carlo (MCMC) iterations. The age-depth models were created based on these sedimentation times and their default prior information. In order to estimate ages for all *sed*aDNA samples, the calibrated age estimates were extrapolated above the depth of the uppermost ^{14}C age (4.5 cm for piston core and 0.5 cm for surface core), and these ages must consequently be treated with caution. Ages were calculated for every 0.5 cm of the cores within pre-defined range limits (piston: 8 – 185.5 cm; surface: 2.5 – 27 cm; Table A, Appendix). Additionally, the piston core's accumulation rates were plotted against age with the function *plot.accrate.age*.

Physical, optical, magnetic and geochemical sediment core properties were obtained from ITRAX scans (Croudace et al. 2006) performed at the Centre for GeoGenetics in Copenhagen. Variations in magnetic susceptibility (Thompson et al. 1975) and elemental profiles in kilo counts per second (kcps) from X-ray fluorescence (XRF) scanning (Kylander et al. 2011; Löwemark et al. 2011) were used as proxies for variations in environmental conditions in the catchment area of the lake (Rothwell et al. 2006; Rothwell & Rack 2006). In total seventeen element profiles were used in statistical analysis to objectively detect stratigraphic clusters and/or to visualise variation patterns in their elemental profiles for interpretation of distinct geochemical properties (Hongve, 1997; Brown et al., 2007; Kylander et al., 2011; Croudace &

Rothwell, 2015). The XRF and magnetic susceptibility (MS) were scanned with 2 and 5 mm intervals, respectively. For comparisons with aDNA sample data in statistical analysis, the values for MS and elemental profiles were averaged over 1 cm, corresponding to the *sed*aDNA sampling interval. The profiles plotted for visual interpretation of variation patterns were modified with a weighted moving average (*pracma* package) to reduce noise, using measurement intervals of ~3 cm for MS and ~2 cm for element ratios.

Table 1: Radiocarbon dates for sediment cores from *Jodavannet* shown with 1σ error, calibrated weighed (w) mean, calibrated median, calibrated 95% confidence age ranges, sample material and sample weight.

Depth (cm)	Core	^{14}C age (BP)	Cal w. mean	Cal. median	Cal 2σ range	Sample material	Sample weight (mg)
3	Surface	112 ± 21	158,9	173,7	-5 – 282,2	Terrestrial MF	1,4
9,5	Surface	519 ± 29	159,7	174,4	-4 – 282,9	Terrestrial MF	0,9
12,5	Piston	279 ± 24	268,2	303	-2 – 426	Terrestrial MF	4,3
27	Surface	196 ± 21	161,5	176,3	-2 – 284,6	Terrestrial MF	2,5
37-38	Piston	767 ± 26	719,7	703,1	655,3 – 891,9	Terrestrial MF	2,2
52-53	Piston	1977 ± 25	1900,7	1900,4	1785,8 – 1998,7	Terrestrial MF	1,3
129	Piston	4968 ± 34	5690,2	5689,3	5426,7 – 5917	Terrestrial MF	0,7
177-178	Piston	9512 ± 40	10696,8	10706,1	10155,6 – 11107	Terrestrial MF	0,9
185-186	Piston	10426 ± 42	11932,4	11912,5	11600,2 – 12340,6	Aquatic MF	2,9

Radiocarbon ages of macrofossils (MF) were calibrated (cal. BP) following IntCal13 (Reimer et al., 2013) using the software Bacon 2.2 with settings specified in Appendix. For samples taken over 1 cm intervals, calibrated ages are given for the intermediate value (±0.5) from the model output.

The profile of MS and ten different elements/element ratios were used to describe climatic variation reflected in the geochemistry of the sediment core. MS was used as proxy for glacial-derived minerogenic input (Snowball & Sandgren, 1996), while Ti indicated detrital sediment input, typically from higher catchment runoff or increased aeorolian deposition (Rothwell & Croudace 2015). The coherent versus incoherent scatter from rhodium (Rh) was used as a density proxy (A. Schomacker, personal communication). To indicate changes in biological production, Ca/Ti and Si/Ti were used because they could indicate biogenic silica production in lakes (Melles et al. 2012; Alsos et al. 2015). The ratio Fe/Mn was also used to reflect enhanced biological productivity, seen as a shift to higher Fe/Mn values caused by anoxic water conditions from organic decay (Kylander et al. 2011).

Several ratio profiles were used to reflect changes in weathering regimes and changes in grain-size of allochthonous material. High K/Al and K/Ti values and low Rb/K values were used to

reflect increased weathering because K is relatively water soluble while Ti, Al and Rb are more stable (Rothwell & Croudace 2015). Al/Si was used to find potential changes in grain-size of distant originated material, because clays are rich in Al while sands are rich in Si (Clift et al. 2014)

SedaDNA extraction, amplification and high throughput sequencing

I extracted sedimental ancient DNA (*sed*aDNA) from 44 subsamples and 6 negative controls at the ancient DNA dedicated laboratories at Tromsø University Museum. Each subsample contained c. 2-5 g sediment. As only the surface core contained material from the undisturbed mud-water interface, the three uppermost subsamples from this core were used to cover the most recent deposited material. The long piston core contained material deposited since the last glacial maximum, making it valuable for investigations throughout the Holocene. Therefore, 41 samples through the whole piston core were chosen for *sed*aDNA analyses, with denser sampling in the deeper layers of the core to focus the investigation on a less studied time-period.

PowerMax Soil DNA Isolation kit (MO BIO Laboratories, Carlsbad, CA, USA) was used for extraction, following the manufacturer's instructions with some modifications. In addition to solution C1, 100 μL of 5 mg/mL proteinase K and 400 μL of 1M dithiothreitol (DTT) were added to each sample. The subsequent vortexing of samples was conducted in a FastPrep-24 TM 5G (M. P. Biomedicals LLC. Santa Ana, CA, USA) for 2x20 seconds at 4,5 m/sec and then incubated at 56°C for *c.* 15 hours. All centrifuge steps were done at 4200 rpm n stead of 2500 rpm. In the end, all samples were recovered in 3 mL elution buffer instead of 5 mL.

All PCRs, subsequent cleaning of amplicons and pooling of amplicons were carried out by Peter Heintzman and Dilli Rijal. The PCR setup was done in a dedicated ancient DNA lab physically isolated from PCR work to prevent contamination from PCR products, and the downstream steps were performed in a PCR lab, both at Tromsø University Museum. Two negative PCR controls (one from the aDNA lab and one from the PCR-lab) and one positive control with synthetically reconstructed sequences were amplified in addition to the 50 DNA extracts from samples and negative controls. The target region was the short P6-loop of the chloroplast *trn*L (UAA) intron (Taberlet et al. 2007), amplified with the universal plant primers *g* and *h*. Unique flanking sequences (*tags*) 8 or 9 base pairs (bp) long were added at the 5' end for sample identification when sequencing multiple samples at once. DNA amplification was conducted in 50 μL final volumes, containing 5 μL of DNA extract, 1X Gold buffer and 2U of AmpliTaq

Gold® DNA Polymerase (Life Technologies, Carlsbad, CA, USA), 2.5mM $MgCl_2$, 0.2mM dNTPs, 0.2µM forward primer, 0.2µM reverse primer and 8µg Bovine Serum Albumin. The PCR mixtures underwent enzyme activation for 10 min at 95°C, followed by 45 cycles of denaturation for 30 sec at 95°C, annealing for 30 sec at 50°C, and elongation for 1 min at 72°C, plus a final elongation step for 7 min at 72°C.

Seven PCR repeats were made per sample to reduce false positives and increase the chance of detecting rare taxa or taxa with low DNA representation in the sediment record (Alsos et al. 2015; Ficetola et al. 2015). PCR-products from all samples and controls were purified using Qiagen MinElute PCR purification kit (Qiagen GmbH, Hilden, Germany), following the manufacturer's instructions. The PCR-products were pooled in Tromsø and sent to FASTERIS (FASTERIS SA, Switzerland) for high-throughput sequencing (HTS). Conversion of the amplicon pool into a library was done according to FASTERIS' MetaFast protocol, which is a PCR-free library preparation. The library was sequenced on an Illumina NextSeq 500 (Illumina, Inc., CA, USA) flow cell sequencing platform, using 2x 150 cycles.

Bioinformatic analyses and taxonomical assignment

I used the OBITools software package (Boyer et al. 2016) to analyse sequence data, and the analysis was run through the Abel computer cluster at the University of Oslo. Amplicons were reconstructed by aligning paired-end reads with *illuminapairedend*, and sequences having lower alignment score than 40 (Alsos et al. 2015) were removed with *obigrep*. The remaining sequences were assigned to samples according to their unique sample tags with *ngsfilter* (demultiplexing), requiring 100% match with tags and maximum 2 bp mismatch in the primer region (default options in OBITools). As *ngsfilter* does not allow different tag lengths, this step was run twice and resulted in two output files that were subsequently merged with the unix *cat* command. Because all tags were unique, sequences with the same forward and reverse tag were considered chimerical sequences between samples, and thus filtered out with *obigrep*. *Obigrep* was also used to remove sequences shorter than 10 bp (Alsos et al. 2015), because this was the minimum threshold for the sequences in the reference databases.

Strictly identical sequences were clustered (dereplication) using *obiuniq*, keeping the information about their distribution among samples. Then sequences with only one copy in the dataset were removed (Alsos et al. 2015) with *obigrep*, before using *obiclean* to tag sequences for detection of potential PCR and sequencing errors. Using information about sequence record counts and sequence similarities across all samples, sequences were classified as *head* (ideally

true sequences), *singleton* (potentially rare true sequences) or *internal* (assumed erroneous sequences)(Boyer et al. 2016). Maximum one bp difference was allowed between two variant sequences, and the abundance threshold ratio for the uncommon *internal* versus common *head* sequence was 5%. This threshold allowed keeping relatively rare sequences, as small sequence differences may make a taxonomical important difference to sequences in the Arctic and boreal database. Sequences with no close resemblance to others (neither *head* or *internal*), were classified as *singleton*. To avoid potential PCR or sequencing errors, only *head* and *singleton* sequences were kept.

Finally, sequences were assigned to taxa based on sequence similarity with two taxonomical reference libraries, using the *ecotag* software (http:// www.grenoble.prabi.fr/trac/OBITools). The reference libraries were obtained from the ECOGEN research group at the Arctic University of Norway, Tromsø. The primary reference library contained local taxa of 815 arctic (Sønstebø et al. 2010) and 835 boreal (Willerslev et al. 2014) vascular taxa in addition to 455 bryophytes (Soininen et al. 2015). The secondary reference library contained sequences from running *ecopcr* on the global EMBL Nucleotide Sequence Database (R134, January 2018). The EMBL reference library was used to assign taxa to sequences without assignment or to get more precise assignment than the primary reference database could achieve. This resulted in two files containing the unique sequences and their taxa assignation from each reference library.

After initial data processing with OBITools, further filtering of the sequences were conducted in R (www.R-project.org, 2017). To avoid any misidentification, only sequences matching 100% to reference library sequences were kept. Next, the two result files were merged, keeping only the arctborbryo-assigned sequence in case of duplicates. To increase confidence in the identified taxa, the kept unique sequences had minimum 10 reads per PCR repeat and minimum two PCR repeats in samples (Alsos et al. 2018). Taxa occurring in negative controls were removed to avoid potential contaminants. In order to exclude potential false positives from the dataset, each taxon had minimum 100 PCR reads in total. Sequences belonging to non-native or marine taxa were blasted with NCBI's BLAST (*Juniperus*, *Cassiope lycopodioides*, *Festuca pratensis*, *Ranunculus sceleratus*, Polypodiales (*Dryopteris filix-mas* or *Gymnocarpium robertianum*) and *Nannochloropsis granulata*; http://www.ncbi.nlm.nih.gov/blast/) to find reasonable explanations for why they were assigned to taxa that were assumed unlikely in the study area. One exotic taxa (*Cedrus*) was a suspected contaminant and therefore removed from the dataset. Finally, some taxa names were modified according to the BLAST-results, accepted taxonomy in *Artsnavnebase* (http://www2.artsdatabanken.no/artsnavn/; 13.06.2018) and their

respective synonyms registered in the Global Biodiversity Information Facility (GBIF.org, 2018).

Vegetation analyses and modern sediment samples: Unsuccessful method calibration

This study intended to conduct a calibration of the method by comparing the relationship of observed vegetation close to the lake and taxa resulting from DNA preserved in the modern lake sediments. For that matter, a thorough vegetation survey was conducted around Jodavannet and several sediment samples were collected from the uppermost sediment layer (Fig. 2). However, due to limited time and unforeseen challenges in the laboratory process, this calibration was unsuccessful. Although the results from this analysis were lacking, I briefly explain the process and its intent, in order to describe the extent of the study and provide useful information to similar future projects.

The vegetation was surveyed 3-5. August 2017, and consisted of point-framing in 120 plots (0.25 m^2) placed in four 30-meter-long transects extending from the edge around the lake close to the sample location of the sediment cores (Fig. 2). The density of the plots were higher closest to the lake, because the flora in this area (< 2 m distance) was expected to be better represented in the sediment records (Alsos et al. 2018). To record vegetation- and ground cover in the plots, first and last hit for all 25 intercepts of the frame were recorded. Vascular plants were identified to species or genus level (Lid & Lid 2005; Rønning 1996), and hits were recorded for the categories bryophytes, lichens and biological crust (thin layer of living material in the uppermost millimetres of soil), litter, open soil and rock. This analysis provided an abundance measure of the vascular plant species and vegetation or ground types, assuming the plots were representative of the vegetation in the area, and that a sufficient number of plots were sampled.

In order to compare the current vegetation with the DNA record from modern lake sediments, five replicates (to account for heterogeneity) from eight samples sites were taken from the uppermost lake sediments in Jodavannet on 8. August 2017. The sample sites aimed to prolong the transects on land towards the point where the sediment cores were sampled.

DNA was extracted using PowerSoil® DNA Isolation kit (MO BIO Laboratories, Carlsbad, CA, USA) following the manufacturer's instructions (version 07272016). Similar to the *sed*aDNA procedure, the universal plant primers *g* and *h* were used with the intention to amplify the P6-loop of the chloroplast *trn*L (UAA) intron (Taberlet et al. 2007) from the extracted DNA. The PCR amplification was unsuccessful, probably due to inhibitors (i.e. humic substances) in

the sediment samples (Wilson 1997). The trouble-shooting attempts dilution and cleaning of DNA-extract were made, but when these were ineffective no further efforts were made due to limited time.

The amplicons would have been sequenced with HTS, and taxon information obtained with OBITools like it was done for the *sed*aDNA data. The plant taxa from the modern sediment record would have been compared with the results from the current vegetation analyses around the lake in order to assess the representation of the current vegetation in the modern lake sediments. This analysis was intended to study how transport, distance and taphonomic processes affect the representation of different plant taxa in DNA records from sediments in a high-arctic lake.

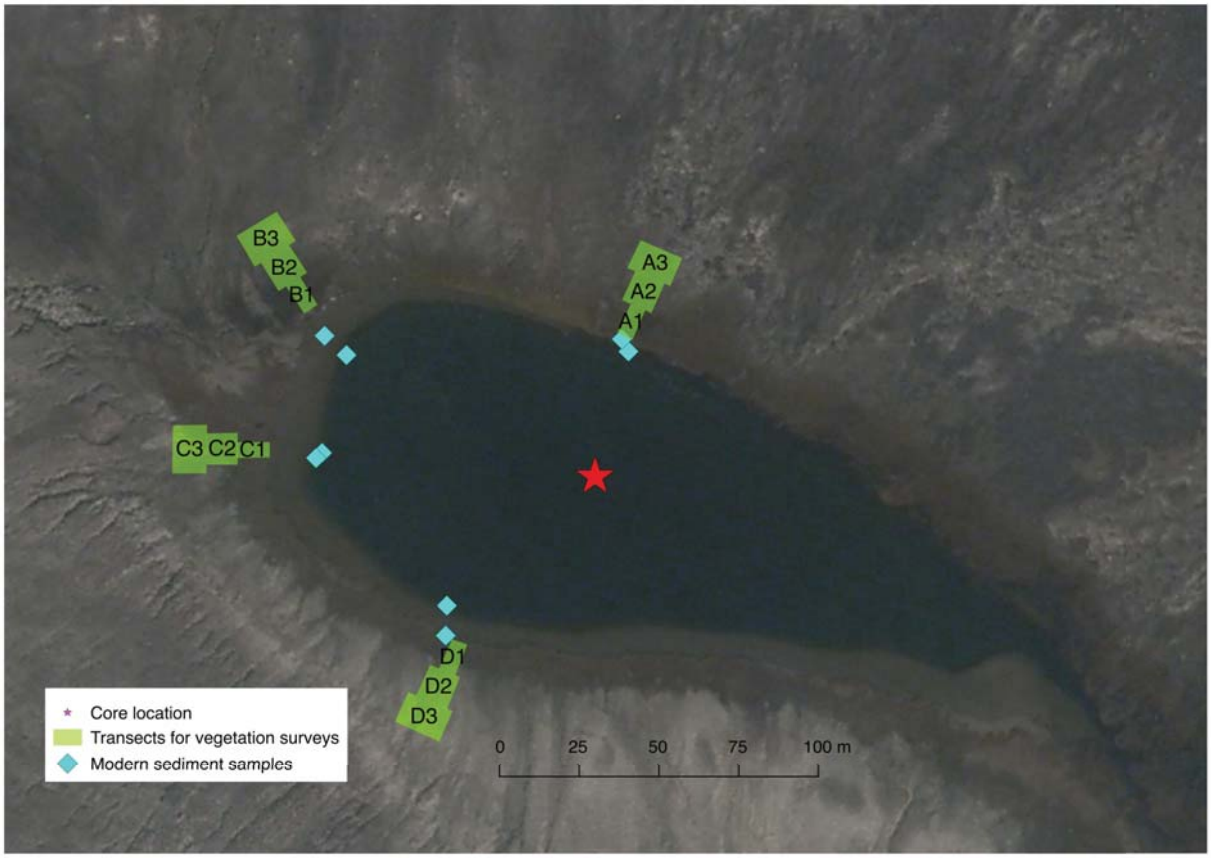

Figure 2: Vegetation survey around Jodavannet. Current vegetation was registered by point-intercept in 0.25 m^2 plots. In total 120 plots from four transects (A-D) divided into three zones were investigated. Ten plots were randomly placed within each zone. The location of the sediment cores used for *sed*aDNA analysis (red star) and sampling locations for modern sediment samples taken for method calibration (blue squares) are marked.

Statistical approach

All statistical analyses were conducted in R (www.R-project.org, 2017). In order to visualise stratigraphic patterns of geochemical variation and identify probable indicators of biological productivity, a principal component analysis (PCA) was conducted on ITRAX-derived data averaged for *sed*aDNA sample intervals and the ordination axis object scores were plotted against core-depth (Legendre & Birks 2012; van der Bilt et al. 2015; Røthe et al. 2015). The PCA was done with R-package *vegan* (version 2.4-4; Oksanen et al. 2017) and the *rda* function. The analysis was performed on MS and sixteen elements (Ti, Si, Ca, S, Fe, Mg, Al, P, K, Mn, Zn, Rb, Sr, Zr, Rh coherent and Rh incoherent), excluding the ones with low detection rates (i.e. many zero-values). Standardized (centred and scaled) values of the PC1 scores were plotted stratigraphically together with standardized values of Ti, Ca/Ti and Si/Ti to investigate if the proxies for biological production reflected lake processes (Røthe et al. 2015).

Finally, to objectively categorize the sediment record into different units, a constrained cluster analysis (package *rioja* 0.9-15.1) with coniss algorithm (Grimm 1987) was applied (van der Bilt et al. 2015). The Euclidian distances of the seventeen standardized ITRAX-variables averaged over *sed*aDNA sampling intervals were used in the analysis. The resulting clusters were plotted stratigraphically with the elemental ratio-plots to depict geochemical variation patterns within the identified zones.

In order to depict the Holocene development of species communities as found by metabarcoding, the *vegdist* function in R-package *vegan* (Oksanen et al. 2017) was used to create a matrix of Bray-Curtis dissimilarity indices of identified unique taxa based on number of PCR repeats per sample. The dataset was modified slightly to capture general trends in similar taxa rather than lowest possible taxonomical resolution, thus species matches within the taxa *Carex*, *Draba*, *Festuca*, Hypnales, *Pedicularis*, Poaeae and three *Saxifraga* species (*cernua*, *hyperborea* and *rivularis*) were grouped together.

The dissimilarity matrix was then clustered with *chclust* function from *vegan*, using constrained hierarchical clustering with clusters constrained by sample depth and the *coniss* algorithm (Grimm 1987). To identify the number of statistically significant groups from the constrained cluster analysis, a broken stick distribution (Bennett 1996) was created with the *bstick* function from the *rioja* package for analysis of Quaternary science data (Juggins 2017). A stratigraphic diagram was created with the *strat.plot* function (rioja) to plot the number of PCR reads of taxa identified from *sed*aDNA samples against the calibrated ages obtained from the age-depth

model. The PCR reads' conservative and relatively unbiased properties made them preferable rather than i.e. counts of PCR reads. The identified clusters from the constrained hierarchical clustering were added to the stratigraphic plot.

Results

Chronology and litostratigraphy

The nine calibrated ages from the AMS radiocarbon dated macrofossils occurred in chronological order in terms of sample depths. The weighed mean calibrated ages for the two cores showed a combined range from 159 to 11932 cal. BP (Table 1). The resulting parameters from the age-depth model run were 36 and 13 vertical sections of 5 and 2 cm thickness for the piston core and the surface core respectively. The calculated ages were based on 8.36 and 3,3 million MCMC iterations for the piston and the surface core, in that order. The relatively stationary and unstructured adjacent iterations indicated a good model run (Fig. A, Appendix).

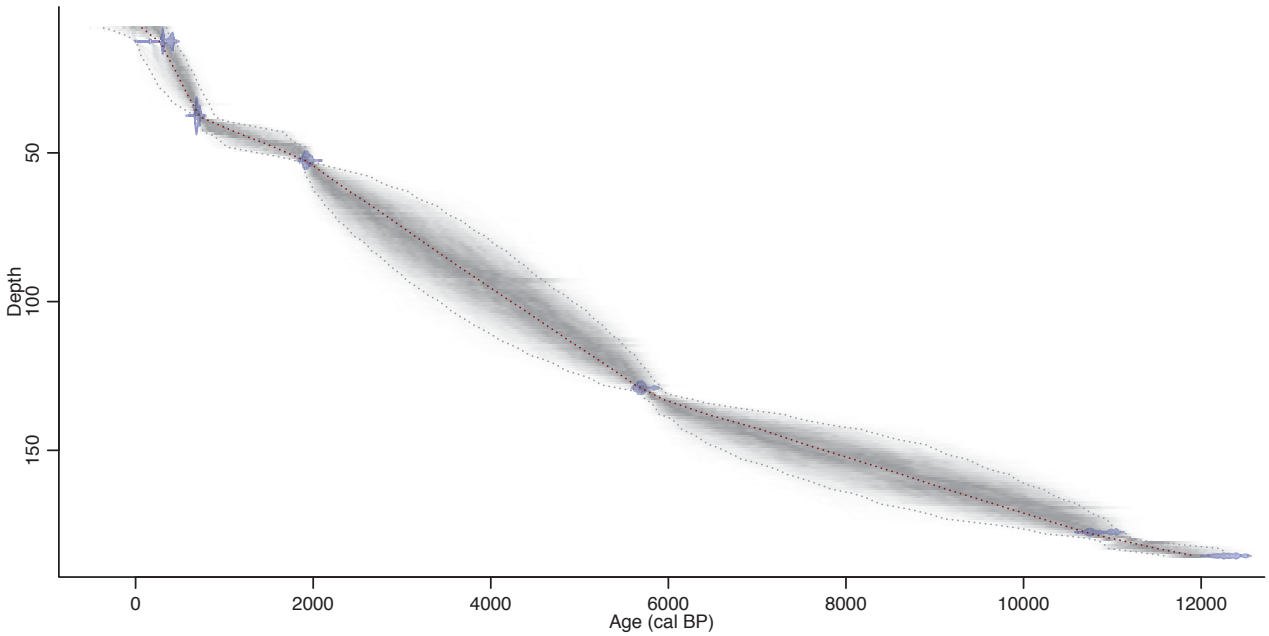

Figure 3: Age-depth model for six calibrated ^{14}C ages (blue) from piston core in *Jodavannet*, Svalbard. The lines show the age-depth curve with the best model from weighted average of the mean (red), more likely calendar ages (darker grey) and the 95 % confidence interval (outer stippled lines). Dates calibrated with IntCal13, model made with Bacon 2.2 with default prior settings and mean sedimentation time (acc.mean) of 50 year/cm, as suggested by the software.

The age-depth model for the piston core indicated a relatively stable accumulation rate over time, but this was a rough representation due to the great timespan between the ^{14}C-dated macrofossils (Fig. 3). The core's accumulation rate was changing during the Holocene, with periods of rapid accumulation (~11500-6000 cal. BP and ~2000-700 cal. BP) separated by more stable accumulation phases (Fig. 4).

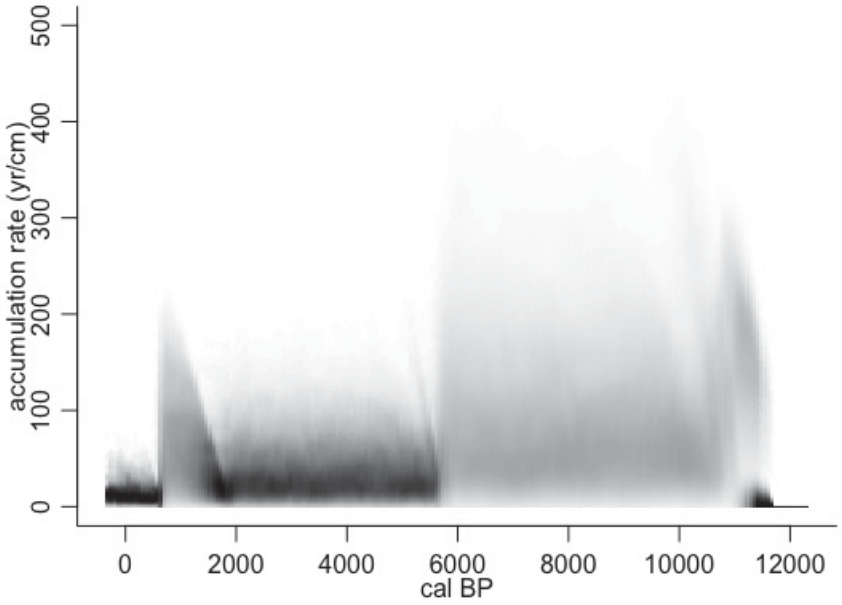

Figure 4: Accumulation profiles for piston core from *Jodavannet*, Svalbard, plotted with Bacon 2.2. Darker grey colour indicates more certain estimates.

Based on the high resolution XRF optical image, elemental ratios and magnetic susceptibility, periodic variations in sedimentation properties and colouration were apparent (Fig. 5), reflecting the changing Holocene environment in the catchment area of the lake. Five stratigraphic zones were identified from the constrained hierarchical cluster analysis on standardized ITRAX-data averaged for *sed*aDNA sample intervals from the piston core (GZ 1-5). The lowest depth in the resulting clusters was 8 cm, because this was the youngest *sed*aDNA sample analysed from the piston core.

GZ 1: Core depth 185-176 cm, c. 11800-10600 cal. BP

The oldest zone was characterized by dense sediments with high values of Ti and K/Al and a peak in MS. These profiles had a sudden decrease towards the zone transition that corresponded with a dark brown layer.

GZ 2: Core depth 175-160 cm, c. 10400-8900 cal. BP

After the preceding drop, Ti, K/Al and Rb/K increased slightly, while MS remained stable and low. The Rb/K profile displayed two subtle peaks, corresponding with similar patterns in Fe/Mn. The ratios for Ca/Ti and Al/Si decreased after the peak during the previous zone transition. Ca/Ti then stabilized, while Al/Si increased slightly throughout the zone. Si/Ti and Fe/Mn had small, almost synchronous rises at ~9000 cal BP.

GZ 3: Core depth 159-90 cm, c. 8700-3800 cal. BP

The profiles for MS and Ti were relatively stable with low values during the whole zone, although Ti had a small increase at *c.* 4,5 ka cal. BP. The profile for Fe/Mn was generally low and stable but had two marked and sudden peaks at approximately 5,4 ka cal. BP.

GZ 4: Core depth 79-48 cm, c. 3200-1600 cal. BP

This zone had in general less stable geochemical profiles than the previous zone. The highest values for MS, density, Ti and K/Al occurred at *c*. 2,8 ka cal BP. Al/Si had relatively high and fluctuating values. Fe/Mn had marked high values during *c.* 2,6 – 2 ka cal. BP, then a drop before a gradual increase towards the transition to the subsequent zone. The first rise in these values corresponded with an unusually high peak in the profiles for Ca/Ti and Si/Ti.

GZ 5: Core depth 39-8 cm, c. 800-90 cal. BP

There was generally more variation in the depicted geochemical patterns in this zone than the first three zones. Big drops occurred at *c.* 900 cal. years BP in the profile for Al/Si. The Si/Ti profile increased at ~2000 cal. BP, while Si/Ti remained almost unchained during that time.

Molecular analysis

The number of sequences and reads resulting from the high-throughput Illumina sequencing was reduced during the OBITools process from initial *c.*16.7 mill. to 7158 unique sequences in *c.*11 mill. reads matched with reference libraries and assigned to taxa. After subsequent fine filtering, there were 78 unique sequences in 2 396 402 reads remaining in the dataset (Table 2). The resulting sequences belonged to vascular plants (74,4 %), algae (6,4 %) and bryophytes (19,2 %) from 68 different taxa in 30 different families (Table 3).

Based on known registrations in Svalbard (Svalbardflora.no and Artskart.no, 13.06.2018) and the BLAST results of the conspicuously assigned taxa, some taxon names were modified from the names originally assigned during the sequence matching with reference databases (Table 3).

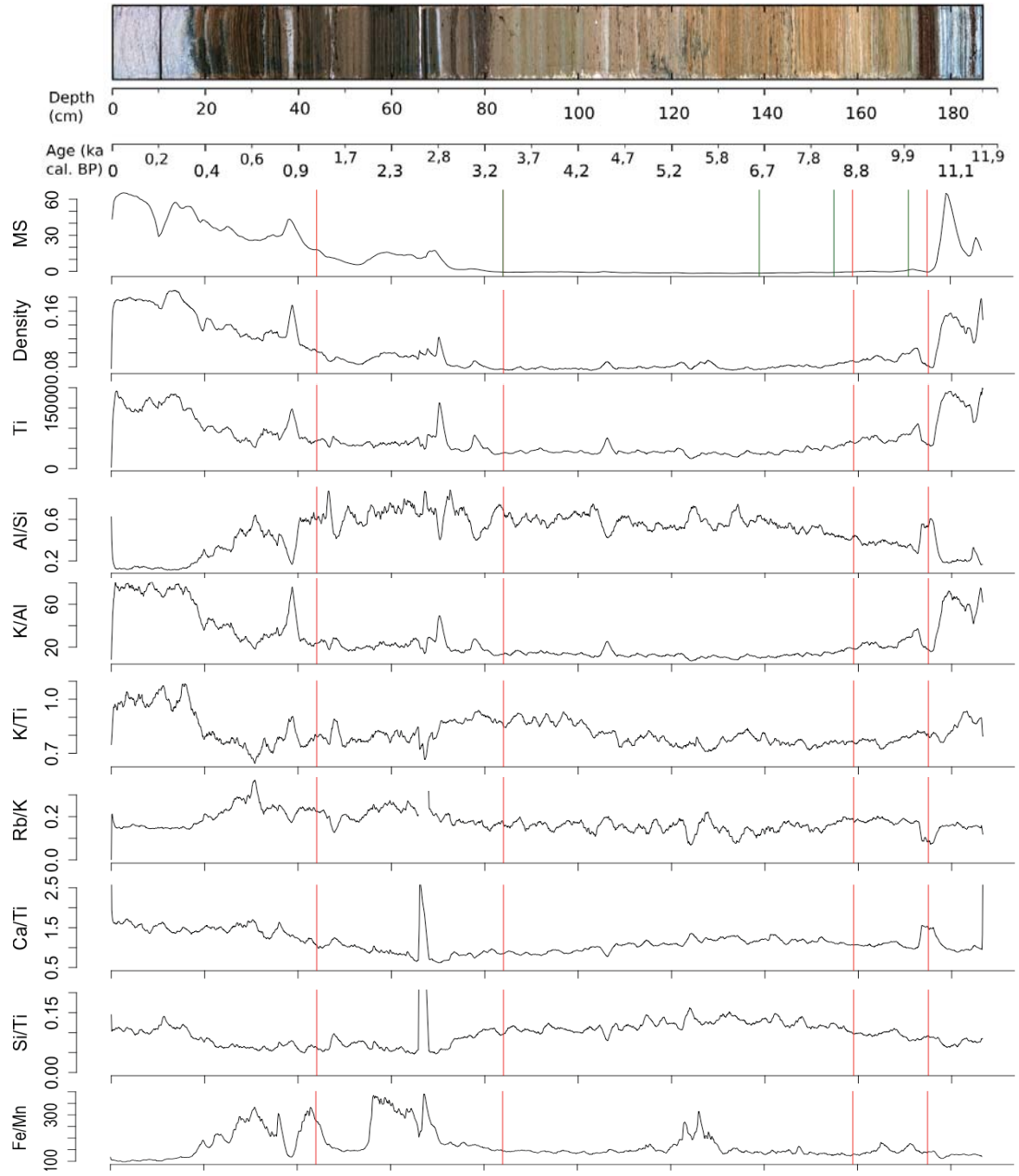

Figure 5: Optical image, magnetic susceptibility (MS), the elemental profiles of Rh coh/Rh inc (density proxy), Ti, Al/Si, K/Al, K/Ti, Rb/K, Ca/Ti, Si/Ti and Fe/Mn (in kcps) obtained from ITRAX-scans of piston core from *Jodavannet*, Svalbard. The weighted moving average of the ITRAX-measurements are plotted against depth on the x-axis, and corresponding age (ka cal. BP) is indicated in a secondary x-axis. The red lines mark the transitions between five clusters identified by constrained hierarchical clustering of MS and sixteen elements averaged over sampling intervals for *sed*aDNA samples from Jodavannet piston core. The green lines in the MS plot, mark identified vegetation clusters for comparison. They derive from cluster analysis on Bray-Curtis distances of PCR repeat abundance of identified taxa in the *sed*aDNA samples from the piston core.

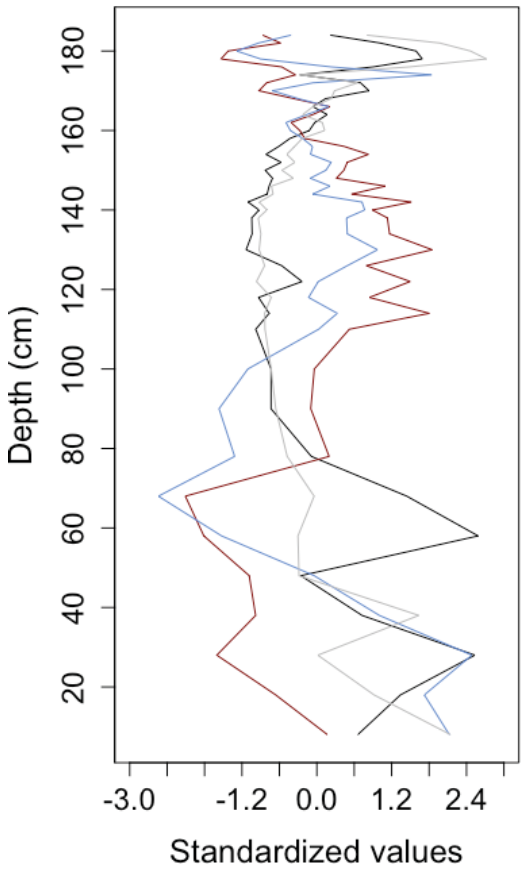

Figure 6: Stratigraphic plot of PC1 scores (black) and element ratios Ca/Ti (blue), Si/Ti (red) and Ti (grey). All values are standardized (scaled and centred).

The ordination axis object scores plotted against core-depth (Fig. 6) revealed a Holocene variation in the geochemical record with the strongest signal in the deepest and shallowest part of the core. The PC1 scores had three peaks at approximately 180, 60 and 30 cm core-depth. The profile of Ti had a relatively uniform variation pattern with the PC1 scores, especially in the deepest sections of the core. The variation patterns of Ca/Ti and Si/Ti compared to the PC1 scores showed an inverse correlation for most of the core stratigraphy. From ~70 cm to 20 cm core-depth, Ca/Ti showed a similar pattern as the plotted PC1 scores, while the Si/Ti variation pattern remained contrasting.

Table 2: Overview of numbers of sequences and reads during the OBITools bioinformatic processing and subsequent fine filtering of sequence data from high-throughput sequencing.

OBITools command	Function	Number of sequences	Number of reads
illuminapairedend	Align forward and reverse reads to reconstruct amplicons	16 666 393	16 666 393
obigrep	Remove badly aligned/reconstructed sequences	16 362 352	16 362 352
ngsfilter	Assign sequeces to samples (demultiplexing)	15 034 086	15 034 086
obigrep	Remove between-sample chimeras	12 921 887	12 921 887
obigrep	Remove sequences shorter than 10 bp	12 782 336	12 782 336
obiuniq	Group identical sequences into a unique sequence with count of sequence read per sample (dereplication)	164 186	12 782 336
obigrep	Remove sequences with low frequency (<2)	50 150	12 668 300
obiclean	Remove PCR and sequencing errors	7 158	11 060 160
ecotag	Assign sequences to taxa	7 158	11 060 160

Only keep sequences matching 100% with arctborbryo database	144	1 822 873
Only keep sequences matching 100% with embl database	167	2 512 450
Merge sequences assigned to taxa from both databases and prioritize arctborbryo in case of duplicate assignment	203	2 641 792
Only keep sequence reads with min. 10 counts per PCR repeat	203	2 636 159
Only keep sequences with presence in samples	140	2 589 720
Only keep sequence reads present in min. 2 PCR repeats per sample/control	92	2 517 911
Only keep sequences without reads in negative controls	87	2 425 788
Group by taxa and remove taxa with <100 reads overall	79	2 425 334
Remove *Cedrus* as possible contaminant	78	2 396 402

No taxa were present in all samples, but overall *Bistorta vivipara*, *Salix*, *Saxifraga* sp. and *Saxifraga oppositifolia* were the most abundant taxa in the *sed*aDNA record from Jodavannet, with presence in more than 50 % of the samples (Table 3). *Dryas*, *Cassiope tetragona* and *Oxyria digyna* were also quite abundant (present in almost 50 % of the samples), followed by *Empetrum nigrum, Potentilla, Equisetum, Papaver, Festuca* and *Draba* (>40 % of the samples).

The stratigraphic plot of the number of PCR repeats in samples for all identified taxa revealed a Holocene development in the species community (Fig. 7). The vegetation in early Holocene (*c.* 12 000 – 10 000 cal. BP) was dominated by moist-dwelling taxa of vascular plants and bryophytes, then transitioned into less bryophytes, more algae and the first occurrences of highly thermophilous taxa like *Arnica* and *Empetrum* and the moderately thermophilous *Huperzia*. From *c.* 8000 cal. BP *Bistorta vivipara* and *Salix* started to dominate the *sed*aDNA record, followed by *Dryas* at *c.* 6000 cal. BP. In the late Holocene (*c.* 3500 cal. BP to present) the species diversity in the record was higher than previous periods, with occurrence of many relatively common vascular plants and bryophytes in Svalbard, but also *Juniperus* (present in one sample with two repeats and 162 reads in total).

Table 3: All taxa from metabarcoding of *sed*aDNA after sequence filtering. Ancient DNA extracted from two sediment cores from *Jodavannet*, Svalbard.

Family	Taxa *sed*aDNA	Sum samples	Max. repeats	Sum repeats	Sum reads	Unique seq. assigned
Asteraceae	***Arnica*** (***angustifolia***)	3	2	4	2212	1 (a)
Asteraceae	*Asteraceae*	6	5	14	1360	1 (a)
Brassicaceae	*Brassicaceae*	1	2	2	2267	1 (b)
Brassicaceae	***Braya*** (***glabella***)	7	6	17	1590	1 (a)
Brassicaceae	***Cardamine*** (***bellidifolia***)	5	5	14	732	1 (a)
Brassicaceae	***Cochlearia*** (***groenlandica***)	3	5	7	2112	1 (a)
Brassicaceae	***Draba*** (***oblongata, arctica***)	8	3	13	4468	1 (a)
Brassicaceae	*Draba*	11	6	24	10289	1 (a)
Caryophyllaceae	***Cerastium*** (***arcticum, alpinum, regelii***)	8	4	15	1072	1 (a)
Caryophyllaceae	*Sabulina* (***Minuartia rubella*** [1])	4	2	5	631	1 (a)
Caryophyllaceae	***Sagina*** (***nivalis, caespitosa***)	6	3	9	1421	1 (a)
Caryophyllaceae	***Silene acaulis***	9	5	17	1920	1 (a)
Caryophyllaceae	***Stellaria*** (***longipes***)	7	6	17	715	1 (a)
Cupressaceae	*Juniperus*	1	2	2	162	1 (a)
Cyperaceae	***Carex*** (***parallela***)	4	5	8	1840	1 (a)
Cyperaceae	***Carex*** (***marina, ursina, glareosa***)	1	2	2	400	1 (a)
Cyperaceae	***Carex*** (***nardina, rupestris***)	8	7	29	1634	1 (a)
Cyperaceae	*Carex*	5	4	12	338	1 (a)
Cyperaceae	***Carex lachenalii***	1	4	4	3316	1 (a)
Equisetaceae	***Equisetum*** (***arvense***)	14	7	26	18198	1 (a)
Equisetaceae	***Equisetum*** (***variegatum, scirpoides***)	11	2	13	1306	1 (a)
Ericaceae	***Cassiope tetragona***	21	18	102	7738	3 (a, b)
Ericaceae	***Empetrum*** (***nigrum***)	15	6	31	23812	1 (a)
Juncaceae	***Juncus biglumis***	7	6	21	3463	1 (a)
Juncaceae	***Luzula*** (***confusa, wahlenbergii, nivalis, arcuata***)	8	7	34	2616	1 (a)
Lycopodiaceae	***Huperzia*** (***arctica***)	2	2	3	2483	1 (a)
Orobanchaceae	*Pedicularis*	5	2	7	246	1 (a)
Orobanchaceae	***Pedicularis*** (***dasyantha, hirsuta***)	6	3	11	616	1 (a)
Papaveraceae	*Papaver*	12	6	35	34638	1 (a)
Poaceae	Agrostidinae (***Calamagrostis neglecta, C. purpurascens***)	2	5	6	176	1 (a)

Poaceae	*Festuca* (***baffinensis, edlundiae, rubra, hyperborea, brachyphylla, ovina***)	11	12	62	10833	2 (a, b)
Poaceae	Poeae (***Phippsia algida***)	6	3	8	1747	1 (a)
Poaceae	Poeae (***Deschampsia sukatschewii***, ***D. cespitosa, D. brevifolia***)	4	4	8	334	1 (a)
Poaceae	Poinae (***Arctophila fulva, Dupontia fisheri***)	9	5	19	1609	1 (a)
Polygonaceae	***Bistorta vivipara***	28	7	140	140128	1 (a)
Polygonaceae	***Oxyria digyna***	21	7	72	26016	1 (a)
Ranunculaceae	***Ranunculus*** (***hyperboreus***)	2	2	3	1051	1 (a)
Ranunculaceae	*Ranunculus sceleratus*	2	4	6	2213	2 (a)
Rosaceae	***Dryas*** (***octopetala***)	21	7	119	238443	1 (a)
Rosaceae	*Potentilla*	13	13	82	46997	2 (a, b)
Salicaceae	Salicaceae (***Salix***)	27	7	139	597242	1 (a)
Saxifragaceae	***Saxifraga*** (***cernua, rivularis, hyperborea***)	13	5	34	10287	1 (a)
Saxifragaceae	*Saxifraga*	28	12	125	29143	5 (b)
Saxifragaceae	***Saxifraga cernua***	12	7	51	9602	1 (b)
Saxifragaceae	***Saxifraga cespitosa***	8	2	10	4540	1 (a)
Saxifragaceae	***Saxifraga oppositifolia***	28	7	125	319508	1 (a)
Saxifragaceae	***Micranthes*** (***hieraciifolia, tenuis*** [2])	11	5	19	1342	1 (a)
Saxifragaceae	***Micranthes*** (***nivalis, tenuis*** [2])	11	3	18	810	1 (a)
	Polypodiales (***Cystopteris fragilis***)	4	6	9	21283	1 (a)
Algae						
Closteriaceae	*Closterium baillyanum*	11	7	32	139979	1 (b)
Desmidiaceae	*Cosmarium botrytis*	20	7	71	23844	1 (b)
Desmidiaceae	*Staurastrum punctulatum*	2	2	3	155	1 (b)
Monodopsidaceae	*Nannochloropsis* sp.	21	7	94	512693	1 (b)
Oocystaceae	*Neglectella solitaria*	4	2	5	357	1 (b)
Bryophytes						
Andreaeaceae	*Andreaea nivalis*	1	2	2	104	1 (a)
Bartramiaceae	Bartramiaceae (***Philonotis tomentella, P. fontana, Conostomum tetragonum***)	5	3	9	163	1 (a)
Bryaceae	Bryaceae (***Bryum arcticum*** [3a], ***elegans*** [3b], ***pseudotriquetrum***)	17	7	43	19918	1 (a)
Bryaceae	Bryaceae (***Plagiobryum zieri*** [4a], ***P. demissum, Bryum wrightii*** [4b])	5	7	16	11746	1 (a)

Bryaceae	*Ptychostomum pallens* (***Bryum pallens*** [5])	4	5	9	1055	1 (a)
Dicranaceae	Dicranaceae (***Dicranum spadiceum, D. fuscescens, D. groenlandicum***)	3	3	6	1358	1 (a)
Ditrichaceae	*Distichium* (***capillaceum, inclinatum***)	9	3	12	1046	1 (a)
Encalyptaceae	***Encalypta*** (***rhaptocarpa, streptocarpa***)	4	2	5	103	1 (a)
Polytrichaceae	Polytrichaceae (**8 species**)	15	7	43	26089	1 (a)
Pottiaceae	Pottiaceae (***Tortella fragilis, Gymnostomum aeruginosum, Hymenostylium recurvirostrum***)	1	2	2	207	1 (a)
Timmiaceae	***Timmia*** (***norvegica, austriaca***)	6	2	9	1844	1 (a)
	Hypnales[6] (**5 species**)	20	17	71	54591	4 (a)
SUM: 30	68			1985	2392151	78

Bold species are known registrations on Spitsbergen (Svalbardflora.no and https://artskart.artsdatabanken.no, 13.06.2018). For DNA sequences matching to several species in the reference libraries, the Svalbard representatives are given in brackets. For some vascular plant- and one algal sequence the taxon name were modified according to BLAST results rather than match with reference databases (*Cassiope lycopodioides* = ***C. tetragona***, *Festuca pratensis* = ***Festuca***, Polypodiales = ***Cystopteris fragilis***, *Nannochloropsis granulata* = *Nannochloropsis* sp.). Letters indicate reference database with 100% sequence match (a=arctborbryo, b=embl).

The scientific names generally origin from matches with the NCBI taxonomy database. In certain cases, the registered names in *Artskart/Artsdatabanken* are synonyms of the names from the NCBI taxonomy database. The listed taxonomic name is then the synonym used in *Artsdatabanken*, not the match from the NCBI taxonomy database: ***Minuartia rubella***[1] = *Sabulina rubella*, ***Micranthes tenuis*** [2] = *Saxifraga tenuis*, ***Bryum arcticum*** **(R.Br.) Bruch & Schimp**. [3a] = *Ptychostomum arcticum*, ***Bryum elegans*** **Nees.** [3b] = *Rosulabryum elegans*, ***Plagiobryum zieri*** **(Hedw.) Lindb.** [4a] = *Ptychostomum zieri*, ***Bryum wrightii*** **Sull. & Lesq.** [4b] = *Ptychostomum wrightii* and ***Bruym pallens*** [5] = *Ptychostomum pallens*. Hypnales[6] is possibly ***Pseudocalliergon turgescens*** (syn. *Drepanocladus turgescens*), **Scorpidium cossonii**, **Tomentypnum nitens**, **Scorpidium revolvens** and/or **Scorpidium scirpoides**.

Five significant stratigraphic zones were found based on the constrained hierarchical cluster analysis of Bray-Curtis community distance on PCR repeats per sample (Fig. 7 and Fig. C, Appendix) and the comparison with a broken stick model distribution (Fig. D, Appendix). The most remarkable distance among adjacent samples was between sample depth 138 and 140 cm (~6600 BP). Then followed the separation of sample depth 170 and 172 cm (~10 000 cal. years BP), 78 and 90 cm (~3500 cal. years BP) and 154 and 156 cm (~8300 cal. BP). These vegetation

zones (VZ1 – VZ5) corresponded with visually marked transitions in the composition of *sed*aDNA taxa (Fig. 7 and Table B, Appendix).

VZ 1: Sample depth 185-172 cm, c. 11800-10200 cal. years BP

This zone was characterised by some species only occurring in the older sediment layers (Pottiaceae, *Ranunculus scleratus* and *Ranunculus hyperboreus*). Most of the taxa dominating in this zone were forbs (herbaceous, non-graminoid flowering plants) and bryophytes typical for wet habitats, e.g. *Ranunculus hyperboreus, Ranunculus sceleratus, Equisetum arvense, Saxifraga (cernua*/*rivularis*/*hyperborea*), Hypnales and Pottiaceae (likely species listed in Table 3). Also, the more dry-adapted taxa *Saxifraga cespitosa, Papaver* and *Cystopteris fragilis* as well as the widely distributed generalist species *Saxifraga oppositifolia* were relatively common in this zone. There were scattered occurrences of *Potentilla sp., Minuartia rubella, Sagina, Bistorta vivipara, Carex sp., Juncus biglumis,* Poaeae*, Cerastium, Draba, Cochlearia groenlandica, Dryas octopetala* and *Micranthes*. Almost 48 % of all *sed*aDNA taxa were found in this zone, with 22 vascular, 8 bryophyte and 2 algae taxa present.

VZ 2: Sample depth 171-156 cm, c. 10000-8500 cal. years BP

The results showed a marked reduction in the common forbs from previous zone (i.e. *Papaver, Potentilla, Cystopteris fragilis* and both *Ranunculus* species are gone), and strong presence of several algae taxa (*Neglectella solitaria, Closterium bayllianum* and *Cosmaryum botrytis* and *Nannochloropsis* sp.). *Equisetum arvense* was less common, whereas *Equisetum scirpoides/variegatum* appeared. The first occurrence of the highly thermophilous taxa *Arnica* and *Empetrum* also appeared in this zone. *Festuca* and *Oxyria digyna* had sparse occurrences, while all the Saxifragaceae species from the previous zone were reduced or absent (*Saxifraga cer/hyp/riv* and *Micranthes*). The taxa diversity was lower than in the previous zone, with 25% of all taxa present: 11 vascular plants, 2 bryophytes and 4 algae.

VZ 3: Sample depth 155-140 cm, c. 8300-6800 cal. years BP

The algae *Nannochloropsis* sp. was still dominating in this zone, whereas the other algae taxa from the previous zone were almost absent. *Empetrum* and *Equisetum scirpoides/variegatum* increased, while *Bistorta vivipara* and *Salix* started to dominate the record. The Saxifragaceae species had a relatively stable presence, and *Silene acaulis* occured for the first time. The overall taxa richness in the record increased slightly, with 28% of all detected taxa (14 vascular, 3 bryophyte and 2 algae).

VZ 4: Sample depth 139-90 cm, c. 6600-3800 cal. years BP

This zone had a consistent presence of *Empetrum*, *Equisetum scirpoides/variegatum*, *Saxifraga oppositifolia*, *Bistorta vivipara*, *Salix* and *Dryas*. *Arnica* was still present, whereas the moderately thermophilious taxa *Huperzia* occured for the first time. *Oxyria digyna* was also relatively common, and *Cassiope tetragona* appeared numerously towards the end of the zone. *Cystopteris fragilis* reappeared sparsely, and *Pedicularis* had its first presence in the record early in this zone. The taxa richness continued to increase, with *c.* 42% of all detected taxa present (22 vascular, 3 bryophytes and 3 algae).

VZ 5: Sample depth 79-2 cm, c. 3200-160 cal. BP

There was a drastic rise in and dominance of graminoid taxa, with increase of *Festuca* and *Carex*. *Juncus biglumis* and Poeae reappeared after absence since VZ1, while *Calamagrostis, Luzula* and Poinae occured for the first time in the record. Among other vascular taxa were only *Huperzia* and *Cystopteris fragilis* lost compared to the previous zone, whereas *Empetrum* had decreased. The remaining non-graminoid taxa were still present in equal or higher repeat abundance compared to the previous zone. Some forbs were appearing for the first time in the record with relatively strong presence (*Stellaria, Cardamine* and *Braya*), while the woody shrub *Juniperus* also occured exclusively in this zone. However, this result should be treated with caution as *Juniperus* was present in only two repeats in one sample in addition to be a 'non-native' taxon not previously registered in Svalbard. The most dominant non-graminoid taxa in this zone were *Papaver*, *Bistorta vivipara*, *Salix, Dryas*, *Pedicularis, Oxyria digyna*, *Cassiope tetragona*, *Potentilla,* and Saxifragaceae. All Saxifragaceae taxa increased from previous zones and had their overall highest repeat abundance in this zone (except *Saxifraga cespitosa*). Several taxa of perennial forbs commonly found in the area today were also relatively abundant in the record from this zone (i.e. *Minuartua rubella, Draba, Cochlearia groenlandica, Silene acaulis, Sagina,* Asteraceae and *Cerastium*). The number of bryophyte taxa increased markedly, with *c.* 92% of the total bryophyte taxa occurring in this zone. Overall, Zone 5 had the highest richness of taxa, with *c.* 75 % of the recorded taxa present (35 vascular, 11 bryophytes and 4 algae).

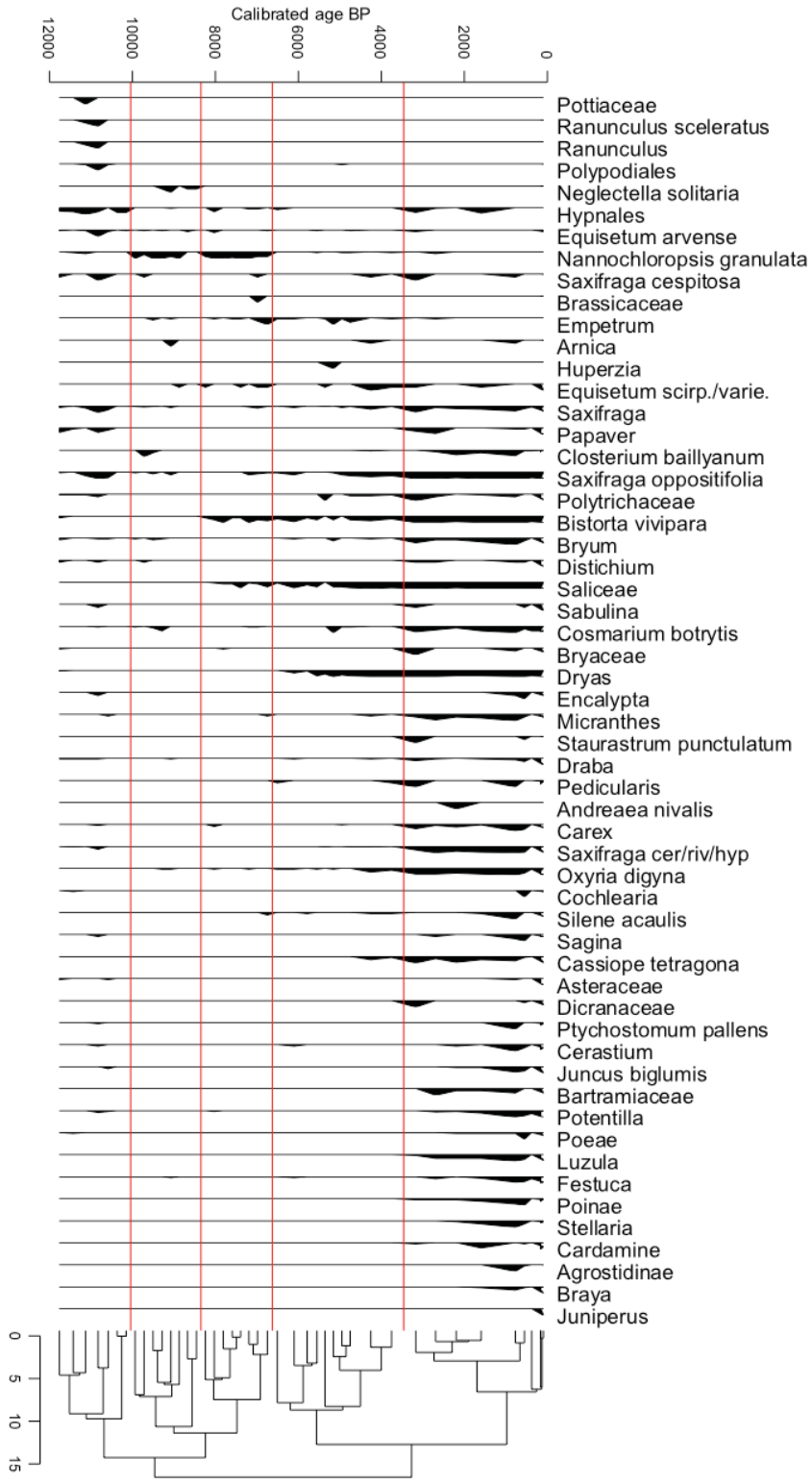

Figure 7: Stratigraphic diagram of vascular plant-, bryophyte and algae taxa identified from ancient DNA. The taxa found in samples from different calibrated ages of the piston core (x-axis) are listed (y-axis) and depicted with abundance measured as number of PCR repeats with taxa sequences present from in total seven repeats per sample (black polygons). The dendrogram (below) is obtained from a constrained hierarchical clustering of species community dissimilarity where clusters are constrained by sample order (depth), and the red lines mark the separation of five significant clusters identified from comparison with a broken stick distribution model. Taxa abbreviated as scirp. (scirpoides), var. (variegatum), cer (cernua), riv (rivularis) and hyp (hyperborea).

Discussion

My result clearly showed that the vegetation in Ringhorndalen has shifted through time since its first establishment about 12 000 years ago. Five stratigraphic zones were identified based on both vegetation data and geochemical data, which were largely congruent. The Holocene *sed*aDNA record reflected early warming and establishment of moist-dwelling taxa and taxa with efficient long-dispersal mechanisms. A transition to colder climatic conditions was evident in both records around 9000 cal. BP, before returning to warmer than present conditions ~8000 cal. BP, reflected in the first occurrence of the thermophilic species *Arnica angustifolia*. The mid-Holocene records indicated relatively dry, warm and stable conditions, with the establishment of several dwarf shrubs and herbs common in Svalbard today. Increased temperature and a transition from moist snow bed communities to dry heath vegetation around 5300 cal. BP was reflected in high species richness and taxa such as *Empetrum nigrum* and *Huperzia arctica*. During the late Holocene, the species richness was at its highest, with persistence of most taxa present earlier in the record. Plant taxa typical for moist sites were dominant from ~3200 cal. BP, whereas a climatic shift towards a drier and warmer climate culminated in a peak at ~2000 cal. BP. Towards the end of the record, a transition to sandy sediments at ~300 cal. BP suggested a broader range of the unique high-arctic steppe vegetation that is prevalent today further away from the studied lake.

Holocene development of vegetation and climate in the catchment area of Jodavannet

The plant taxa recorded from *sed*aDNA in the ~12 000 years old sediment core revealed a Holocene transition in vegetation composition that was divided into five stratigraphic zones (Fig. 7). Five zones were also identified from the geochemical ITRAX-data averaged over *sed*aDNA sample intervals (Fig. 5). Most identified zones were matching, whereas one vegetational zone transition (~6800 cal. BP) and one geochemical zone transition (~800 cal. BP) were absent in the cluster analysis of the other data record.

Early Holocene warming, followed by cooling (11800 – c. 8500 cal. BP)

The two oldest zone transitions identified from both vegetation and geochemistry were almost identical. The geochemical record of the oldest zone (~11800 – 10200 cal. BP) depicted dense sediments with high values of Ti, K/Al and MS, likely reflecting high input of minerogenic material from retreating glaciers due to higher temperatures in the early Holocene Salvigsen & Høgvarde 2006; Mangerud & Svendsen 2018). The *sed*aDNA records was characterized by a relatively species rich plant assemblage indicating a diverse habitat selection for the first

colonists in the early Holocene. Most of the dominating taxa were typical for moist sites i.e. *Ranunculus, Micranthes, Equisetum arvense* and several bryophyte taxa (Pottiaceae, Hypnales, Polytrichaceae and *Bryum*). This might reflect the fact that one of the main dispersal routes was with drift wood from large rivers in Siberia (Alsos et al. 2007), making moist-dwelling taxa more likely passengers for long-distance dispersal.

The overall plant assemblage from this period indicated several vegetation types including dry scree slopes with favourable exposition (*Draba, Potentilla, Saxifraga* and *Cystopteris fragilis*), snow beds with *Phippsia algida* (seen as early occurrence of Poaeae in Figure 7) and *Ranunculus* (Elvebakk 1994), and zonal vegetation typical of the high arctic polar desert characterized by *Papaver, Saxifraga* (*oppositifolia*, *cernua* and *cespitosa*), *Phippsia algida, Draba* spp. and *Cerastium* (Daniëls et al. 2016). The relatively diverse plant community assemblage documented in the *sed*aDNA record from this zone, is in accordance with Bennike and Hedenäs (1995), suggesting an early Holocene establishment of modern flora in Svalbard. Additionally, a typical common feature for the earliest recorded species is effective long-distance dispersal mechanisms such as small, light seeds/spores (i.e. *Papaver*, bryophytes), wind-pollination (i.e. *P. algida*) or self-pollination (i.e. *Saxifraga*), making them successful early colonizers.

The transition into the second oldest zone (*c.* 10200 – 8500 cal. years BP) was marked by a sudden decrease in indicators of detrital input (Ti, MS, K/Al) that corresponded to a dark brown sediment layer typical of organic material. Additionally, there was a marked increase in Ca/Ti, which is a proxy for biogenic silica productivity (Alsos et al. 2015). Because Ca/Ti showed an inverse correlation with the main drivers of the geochemical signal (Fig. 6), this profile is likely to reflect Ca from lake processes rather than from sediment input, such as evaporative concentration or biogenic production. The increase in Ca/Ti was in accordance with the high occurrence of algal taxa found in the *sed*aDNA record at this time, indicating favourable conditions for biological productivity in the lake. The drop in Rb/K and slight rise in K/Ti visible at the zone transition, is typical for increased weathering. The corresponding peak in Al/Si, characteristic for clay-rich sediments, combined with a decrease in minerogenic glacier-derived input indicates that the increased weathering was due to a wetter climate. Wetter conditions around 10000 cal. years BP was reflected in a reduction in drought tolerant species like *Papaver*, *Potentilla* and *Cystopteris fragilis* in the *sed*aDNA record. A continuous domination of algae taxa and the first occurrences of highly thermophilous arctic species (*Arnica angustifolia* and *Empetrum nigrum* around 9500 cal. years BP), combined with

decreased signals of weathering from wet climate (increased Rb/K and decreased K/Ti and Al/Si), indicated still warm but drier conditions throughout this zone. The early record of thermophilous species not commonly distributed around Svalbard today is in line with the description of a first Holocene warm period in Svalbard with climate about 6°C warmer than present between 10 and 9,2 cal. ka BP (Mangerud & Svendsen 2018).

There was a marked drop of plant taxa richness in the sample depth corresponding to c. 8900 cal. years BP, and *Empetrum* and *Arnica* disappeared from the record. This corresponds to a cooler Holocene period between c. 9000 and 8200 cal. BP (Mangerud & Svendsen 2018). Plant taxa richness increased and *Empetrum* reappeared at *c.* 8000 cal. years BP, in line with the return to warmer than present conditions at *c.* 8000 cal BP (Mangerud & Svendsen 2018). There were small peaks in the profiles of Si/Ti and Fe/Mn around this time, probably reflecting increased biogenic silica productivity from lake processes (similar to Ca/Ti; Fig. 6) in the lake and an onset of anaerobic conditions caused by enhanced organic decay.

Dry and warm in the middle Holocene (8500 – c. 3400 cal. BP)

A third vegetation zone was identified at c. 8500 – 6500 cal. years BP, but this was absent in the geochemical analysis. The clustering of this vegetation zone seemed to be highly influenced by algal taxa, especially *Nannochloropsis* sp. High overall algal productivity during 8100-6600 cal. BP has previously been interpreted from diatom concentrations from a lake in western Spitsbergen (Holmgren et al. 2010). This finding co-occurred with a sediment record indicating high biological productivity driven by warmer growing seasons and/or shorter ice covered periods in the same study area (Alsos et al. 2015). Main drivers of the geochemical signal in lake sediments are typically elements connected to inorganic detrital input to the lake (Røthe et al. 2015), meaning element profiles connected to lake processes are not likely to have a strong contribution to the overall variation in the geochemical data. Assuming *Nannochloropsis* blooms caused by favourable conditions in the lake were driving the identified vegetation cluster, this signal was not likely to be captured in the geochemical record in this study.

Apart from the algal dominance causing the vegetation transition at *c.* 6500, the zones resulting from the two different cluster analyses were almost identical for the middle Holocene (*c.* 8500 – 3400 cal. years BP). *Salix* and *Bistorta vivipara* dominated the vegetation from around 8000 cal. BP, until *Dryas octopetala* and *Saxifraga oppositifolia* established around 6000 cal. BP. This reflects increasing summer temperatures with a transition from moist snowbed communities to semi-dry heath vegetation (Elvebakk 1994). The geochemical signals showed

relatively low and stable detrital and minerogenic input (Ti, MS), reflecting dry conditions, with an increased anoxic depositional environment (peak in Fe/Mn) at around 5300 cal. BP probably caused by the enhanced biological productivity reflected in the vegetation (high taxa richness and an increase in thermophilic taxa like *Empetrum* and *Huperzia*). This corresponds to a warm Holocene climate in Svalbard with especially high temperatures occurring from 5500-5000 cal. BP, as suggested by Luoto et al. (2017).

The subsequent establishment of *Cassiope tetragona* around 4300 cal. BP indicates less exposed winter conditions, because this species is sensitive to frost movements of the ground and dependent on some snow cover during winter (Rønning 1996). However, the appearance of *C. tetragona* at this point does not imply that the preceding climatic conditions were unfavourable for the species to establish. *C. tetragona* probably had refuge far away from Svalbard, in Beringia, during the last glaciation. Then it dispersed all the way through the Arctic to Svalbard after deglaciation (Eidesen et al. 2007). The corresponding presence of *Oxyria digyna*, typically confined to moist/wet habitats (Rønning 1996), is supporting the idea of changing climate. Also, the increased profiles of K/Al and Ti, reflecting more weathering and higher catchment run-off, indicates wetter conditions which support the overall trend seen in the *sed*aDNA record.

A persistent species-rich flora in the late Holocene, (c. 3200 – c. 100 cal. BP)

The latest part of the Holocene was included in one identified vegetation zone (*c*. 3200-160 cal. BP) and two identified geochemical zones (*c.* 3200-1600 cal. BP and *c.* 800-90 cal. BP). Both geochemical zones during the late Holocene were characterised by increased detrital input to the lake compared to the mid-Holocene (higher values of MS, Ti, density, K/Al and K/Ti), but the sediment properties seemed to vary between sand (low Al/Si values) and clay (high Al/Si values). The clay-rich periods were assumingly influenced by run-off due to wet climatic conditions, indicated in the *sed*aDNA record by more cold-adapted and moist snow bed communities from around 3200 cal. BP, characterised by *Pedicularis, Luzula* and *Cardamine bellidifolia* (Elvebakk 1994; Hadač 1989). Establishment of the typical wetland/ mire species *Arctophila fulva/Dupontia fisheri* (Elvebakk 1994) also supports this assumption. The climatic shift observed in the *sed*aDNA record corresponds with a cooling episode found at ~3300 cal. BP in chironomid sequences and isotope records from lake sediments on the south-west coast (Luoto et al. 2017) as well as in glacial reconstructions of Karlsbreen glacier on the north-west coast of Svalbard (Røthe et al. 2015).

Subsequent consistent records of more dry-adapted taxa like *Draba*, *Dryas* and *Andreae nivalis*, as well as the thermophilous taxa *Empetrum*, *Arnica* and *Calamagrostis*, indicates a catchment area in the late Holocene that comprised a diverse mosaic of vegetation communities. The mentioned thermophilic taxa combined with the strong occurrence of algal species in this zone (~92 % of total taxa present in the *sed*aDNA record in relatively many PCR repeats) is in accordance with assumed warm Holocene conditions around 2000 cal. BP (Luoto et al. 2017), which is reflected in an increase in biological productivity in the lake (increased Si/Ti). Ca/Ti does not reflect the same pattern, but considering the variation pattern of Ca/Ti compared to the stratigraphically plotted PC1 scores (Figure 6), the signal from Ca/Ti does not strongly reflect lake processes at this core depth, like Si/Ti seems to do. The most recent occurrence of a thermophilic species in the record was *Arnica angustifola* at ~770 cal. BP, indicating the beginning of the little ice age in Svalbard around 700-800 cal BP (Luoto et al. 2017)

In general, the late Holocene *sed*aDNA records revealed a relatively species rich flora (presence of ~75% of all detected plant taxa), with persistence/reestablishment of taxa from the early Holocene record in addition to new taxa occurrences. This is in line with a similar study from western Spitsbergen that found almost all taxa from a Holocene *sed*aDNA record to persist after 4200 cal. BP (Alsos et al. 2015). In the record from Jodavannet, only four taxa from earlier zones were absent in the youngest of the identified vegetation zones (*Cystopteris fragilis, Huperzia arctica, Ranunculus hyperboreus* and *R. sceleratus*).

The transition to sandy sediments at *c.* 300 cal (low Al/Si). BP that prevailed for the remaining part of the piston core's stratigraphy, suggests a historically broader distribution of the high-arctic steppe vegetation that are common in the outskirts of Ringhorndalen today. In accordance to this were typical taxa for this vegetation type that do not currently exist in close proximity to the lake found in the *sed*aDNA record (*Potentilla*). Additionally, during the surveys of current vegetation, observations were made about the distinct ground cover on the southern side of Jodavannet, indicating early succession with a thin biological crust layer on top of a sandy substrate.

Recent dispersal or relict survival?

Ringhorndalen houses several unusual and thermophilous plant population seen in a local and/or high arctic context. A question raised by previous studies that I aimed to address was whether these remarkable plant populations are remnants from a Holocene warm period when

conditions in Svalbard were more favourable for plant growth (Eidesen et al. 2013; Elvebakk & Nilsen 2016) (Eidesen et al, unpublished)? Although none of the most remarkable species in question (*Pinguicula alpina, Festuca ovina, Luzula spicate* and *Erigeron uniflorus*) were confidently discovered in the vegetation reconstruction from Jodavannet, the results reflect local conditions that were warmer than present and establishment of highly thermophilic species (*Empetrum nigrum* and *Arnica angustifolia*) during the early Holocene (~9500 cal. BP). The occurrence of these species in the *sed*aDNA record indicates that their populations persisted locally during several cooler climate periods (~9000-8200 cal. BP and ~3300 cal. BP), by consistently reappearing in the record during the warmer periods around 5300 cal. BP (*Huperzia arctica* also present) and ~2000 cal. BP. The last appearance of *Arnica* in the *sed*aDNA record was at ~770 cal. BP, corresponding with the initiation of the little ice age in Svalbard around ~700-800 cal. BP (Luoto et al. 2017). Today *Arnica* and *Empetrum* have sparse occurrences in Ringhorndalen, and *Huperzia* is rare (Eidesen et al., unpublished), and none of them are likely to be found within the catchment area of Jodavannet. Their local range seems delimited to further into the valley where conditions are warmer and more sheltered. The overall pattern these highly thermophilic species display in the Holocene vegetation record indicates favourable climatic conditions that facilitated a broader local distribution range during the warmest times in the Holocene, and local persistence with reduced range during colder periods. These findings are in accordance with the hypothesis of Holocene survival in Ringhorndalen, but ongoing phylogenetic studies on selected species will give more answers to this question (Eidesen et al., unpublished).

Future prospects for the vegetation development in Ringhorndalen

The Holocene vegetation in the catchment area of Jodavannet that resulted from the *sed*aDNA record reflected the climatic conditions at the time. Assuming anticipated future warming in Svalbard of at least 2°C (IPCC 2013; Monitoring 2012) and an expected increase in Arctic precipitation, mostly as rain (Bintanja & Andry 2017), this record contains climatic analogues that to some extent could be used to predict the species composition in the study area. Arctic ecosystems are expected to respond rapidly to warming, and the main change is expected to be in production and biomass rather than on biodiversity (Gajewski 2015), making the non-quantitative method applied in this study unsuitable to predict change. Additionally, the reconstructed vegetation from *sed*aDNA records represents more than climate. The relatively young arctic biome has gone and is still going through a colonization process. The Svalbard flora is relatively small, even in an arctic context, indicating that the reason why species with

an arctic distribution that still do not exist in Svalbard is simply because they have not successfully expanded their range to the archipelago yet. Often is the establishment phase the limiting factor for successful colonization rather than the dispersal (Alsos et al. 2007). Stochastic dispersal events require some luck and the suitable dispersal mechanisms (Nathan et al. 2006; Nathan et al. 2008) Similarly, is *Bombus* absent in Svalbard, but presence in high Arctic Greenland shows that climate is not the limiting factor. Dispersal of effective insect pollinators to Svalbard could possibly ease the colonisation phase for species 'waiting' to establish (Eidesen et al. 2017). Thus, the response to future climate change cannot be interpreted directly from the vegetation record, but must be seen as a recolonization process that, especially in early stages, reflects the accumulation of species resulting from random long-distance dispersal, stochastic events, dispersal- and reproduction mode.

False positives?

The plant taxa reflected in the *sed*aDNA record must be interpreted with caution, because false positives can occur from degraded DNA and PCR/sequencing errors (Ficetola et al. 2016). The conservative options applied during the bioinformatic filtering process (i.e. 100 % match with reference sequences, minimum 10 reads per PCR repeat and two PCR repeats in samples for unique sequences, and minimum 100 PCR reads per taxa), combined with good knowledge about current plant species occurrences in the area and the Svalbard flora, enabled me to infer confident patterns of Holocene vegetational change in the catchment area. There was however, two assigned taxa that had to be assessed more carefully than others in order to falsify or accept them as probable sequences.

Ranunculus sceleratus is not previously described for Svalbard, and this result should be interpreted cautiously. However, the result seems plausible with presence in two subsequent samples and six PCR repeats in total (4 repeats for one sample; Table 3), and no likely explanation regarding false taxonomical assignation of the sequences found with BLAST. Several registrations of species new to Svalbard have been made in Ringhorndalen previously, making it easier to imagine that more uncommon arctic species have existed in the area.

Juniperus is a less realistic result, with relatively low read counts (162) in two PCR repeats in only one sample (Table 3). The sequence occurred in a relatively modern sample, which I consider unlikely for a taxon with its current distribution range in the low Arctic. A plausible explanation is that *Juniperus* is a false positive result, which is known to commonly occur with high-throughput sequencing (Ficetola et al. 2016). Alsos et al. (2018) found a posterior

probability of 6 – 33 % for a false positive to be present in DNA records from the studied lake sediments in northern Norway and identified probable sources of error to be drop contamination from adjacent samples during PCR or sequencing errors caused by small variations (e.g. 1 base pair) between true and false sequences. For the *Juniperus* sequence from Jodavannet, contamination is a very likely explanation because the samples were processed and sequenced in the same facilities and using the same equipment as samples from northern Norway.

Conclusion

The Holocene vegetation reconstructed from *sed*aDNA for the catchment area of a high-Arctic lake in Ringhorndalen, Svalbard, clearly showed patterns of variation in terms of species assemblages, species richness, and ecological niche preferences. The identified patterns were corresponding to geochemical proxies reflecting variations in glacial melting, erosion and weathering regimes, changes in grain-size of allochthonous material and biological productivity within the lake. The marked shifts between warmer and colder temperature regimes reflected in the two local records combined, were in accordance with main climatic shifts on Svalbard identified by previous studies. These were a cooling event at ~8900 cal. BP and subsequent warming around 8000 cal. BP (Mangerud & Svendsen 2018). Then followed another marked temperature rise ~5300 (Luoto et al. 2017), before cooling at ~3300 cal. BP (Røthe et al. 2015; Luoto et al. 2017). The final main climatic shifts detected in this record were a marked temperature increase ~2000, and finally a cooling period at about 770 cal. BP, assumingly the onset of the little ice age (Luoto et al. 2017).

The early Holocene had a relatively species rich flora, with dominant species typical for moist habitats, possibly due to the main dispersal routes to Svalbard from Siberian rivers. The number of taxa recorded decreased drastically during the first cooling event (~8900 cal. BP), but increased gradually towards ~2000 cal. BP, reflecting the variable dispersal mechanisms and time needed for postglacial re-colonization of different Arctic species. Thermophilic species like *Arnica angustifolia*, *Empetrum nigrum* and *Huperzia arctica* occurred sporadically throughout the record from ~8000 cal. BP to ~770 cal. BP, suggesting that they had broader local distribution ranges extending into the catchment area of the lake during the Holocene warm periods. This finding supports the hypothesis that isolated populations of unusually thermophilic plant species found in Ringhorndalen today, are relicts from a warmer more widespread distribution during warmer periods in the Holocene.

Bibliography

Allen, J. R. M. & Huntley, B. (1999). Estimating past floristic diversity in montane regions from macrofossil assemblages. *Journal of Biogeography*, 26 (1): 55-73. doi: DOI 10.1046/j.1365-2699.1999.00284.x.

Alsos, I. G., Eidesen, P. B., Ehrich, D., Skrede, I., Westergaard, K., Jacobsen, G. H., Landvik, J. Y., Taberlet, P. & Brochmann, C. (2007). Frequent long-distance plant colonization in the changing Arctic. *Science*, 316 (5831): 1606-1609.

Alsos, I. G., Sjögren, P., Edwards, M. E., Landvik, J. Y., Gielly, L., Forwick, M., Coissac, E., Brown, A. G., Jakobsen, L. V., Føreid, M. K., et al. (2015). Sedimentary ancient DNA from Lake Skartjørna, Svalbard: Assessing the resilience of arctic flora to Holocene climate change. *The Holocene*, 26 (4): 627-642. doi: 10.1177/0959683615612563.

Alsos, I. G., Lammers, Y., Yoccoz, N. G., Jorgensen, T., Sjogren, P., Gielly, L. & Edwards, M. E. (2018). Plant DNA metabarcoding of lake sediments: How does it represent the contemporary vegetation. *PLoS One*, 13 (4): e0195403. doi: 10.1371/journal.pone.0195403.

Balascio, N. L., Zhang, Z., Bradley, R. S., Perren, B., Dahl, S. O. & Bakke, J. (2011). A multi-proxy approach to assessing isolation basin stratigraphy from the Lofoten Islands, Norway. *Quaternary Research*, 75 (1): 288-300.

Bennett, K. D. (1996). Determination of the number of zones in a biostratigraphical sequence. *New Phytologist*, 132 (1): 155-170.

Bennike, O. & Hedenäs, L. (1995). Early Holocene land floras and faunas from Edgeøya, eastern Svalbard. *Polar Research*, 14 (2): 205-214.

Bintanja, R. & Andry, O. (2017). Towards a rain-dominated Arctic. *Nature Climate Change*, 7 (4): 263.

Birks, H. H. (1991). Holocene vegetational history and climatic change in west Spitsbergen-plant macrofossils from Skardtjørna, an Arctic lake. *The Holocene*, 1 (3): 209-218.

Birks, H. H., Paus, A., Svendsen, J. I., Alm, T., Mangerud, J. & Landvik, J. Y. (1994). Late Weichselian Environmental-Change in Norway, Including Svalbard. *Journal of Quaternary Science*, 9 (2): 133-145. doi: DOI 10.1002/jqs.3390090207.

Blaauw, M. & Christen, J. A. (2011). Flexible paleoclimate age-depth models using an autoregressive gamma process. *Bayesian Analysis*, 6 (3): 457-474. doi: 10.1214/ba/1339616472.

Boyer, F., Mercier, C., Bonin, A., Le Bras, Y., Taberlet, P. & Coissac, E. (2016). obitools: a unix-inspired software package for DNA metabarcoding. *Molecular Ecology Resources*, 16 (1): 176-82. doi: 10.1111/1755-0998.12428.

Briner, J. P., Stewart, H. A. M., Young, N. E., Philipps, W. & Losee, S. (2010). Using proglacial-threshold lakes to constrain fluctuations of the Jakobshavn Isbræ ice margin, western Greenland, during the Holocene. *Quaternary Science Reviews*, 29 (27-28): 3861-3874. doi: 10.1016/j.quascirev.2010.09.005.

Clift, P. D., Wan, S. & Blusztajn, J. (2014). Reconstructing chemical weathering, physical erosion and monsoon intensity since 25 Ma in the northern South China Sea: a review of competing proxies. *Earth-Science Reviews*, 130: 86-102.

Croudace, I. W., Rindby, A. & Rothwell, R. G. (2006). ITRAX: description and evaluation of a new multi-function X-ray core scanner. *Special Publications*, 267 (1): 51-63. doi: 10.1144/GSL.SP.2006.267.01.04.

Croudace, I. W., & Rothwell, R. G. (Eds.). (2015). *Micro-XRF Studies of Sediment Cores: Applications of a non-destructive tool for the environmental sciences* (Vol. 17). Springer.

Daniëls, F. J., Elvebakk, A., Matveyeva, N. V. & Mucina, L. (2016). The Drabo corymbosae-Papaveretea dahliani– a new vegetation class of the High Arctic polar deserts. *Hacquetia*, 15 (1): 5-13.

Eidesen, P. B., Carlsen, T., Molau, U. & Brochmann, C. (2007). Repeatedly out of Beringia: Cassiope tetragona embraces the Arctic. *Journal of Biogeography*, 34 (9): 1559-1574.

Eidesen, P. B., Strømmen, K. & Vader, A. (2013). Fjelltettegras Pinguicula alpina funnet ny for Svalbard i Ringhorndalen. *Blyttia*, 71 (4): 209-213.

Eidesen, P. B., Little, L., Müller, E., Dickinson, K. J. & Lord, J. M. (2017). Plant–pollinator interactions affect colonization efficiency: abundance of blue-purple flowers is correlated with species richness of bumblebees in the Arctic. *Biological Journal of the Linnean Society*, 121 (1): 150-162.

Elvebakk, A. (1994). A survey of plant associations and alliances from Svalbard. *Journal of Vegetation Science*, 5 (6): 791-802.

Elvebakk, A. & Nilsen, L. (2002). Indre Wijdefjorden med sidefjordar: eit botanisk unikt steppeområde. *Rapport til Sysselmannen på Svalbard*. University of Tromsø, Tromsø.

Elvebakk, A. (2005a). 'Arctic hotspot complexes' – proposed priority sites for studying and monitoring effects of climatic change on arctic biodiversity. *Phytocoenologia*, 35 (4): 1067-1079. doi: 10.1127/0340-269x/2005/0035-1067.

Elvebakk, A. (2005b). A vegetation map of Svalbard on the scale 1:3.5 mill. *Phytocoenologia*, 35 (4): 951-967. doi: 10.1127/0340-269x/2005/0035-0951.

Elvebakk, A. & Nilsen, L. (2016). Stepperøyrkvein Calamagrostis purpurascens i Wijdefjorden på Svalbard - einaste lokalitetar i Europa. *Blyttia*, 74: 259-266.

Farnsworth, W. R., Schomacker, A. & Ingólfsson, Ó. (2016). *Holocene history of Svalbard ice caps and glaciers*: The Carlsberg Foundation. Available at: http://www.carlsbergfondet.dk/en/Research-Activities/Research-Projects/Other-Research-Projects/Anders-Schomacker_Holocene-History-of-Svalbard-Ice-Caps-and-Glaciers (accessed: 29.01.2018).

Ficetola, G. F., Pansu, J., Bonin, A., Coissac, E., Giguet-Covex, C., De Barba, M., Gielly, L., Lopes, C. M., Boyer, F. & Pompanon, F. (2015). Replication levels, false presences and the estimation of the presence/absence from eDNA metabarcoding data. *Molecular Ecology Resources*, 15 (3): 543-556.

Ficetola, G. F., Taberlet, P. & Coissac, E. (2016). How to limit false positives in environmental DNA and metabarcoding? *Molecular ecology resources*, 16 (3): 604-607.

Gajewski, K. (2015). Impact of Holocene climate variability on Arctic vegetation. *Global and Planetary Change*, 133: 272-287. doi: 10.1016/j.gloplacha.2015.09.006.

GBIF.org (2018), *GBIF Home Page*. Available from: https://www.gbif.org [13th June 2018].

Gjerde, M., Bakke, J., D'Andrea, W. J., Balascio, N. L., Bradley, R. S., Vasskog, K., Ólafsdóttir, S., Røthe, T. O., Perren, B. B. & Hormes, A. (2017). Holocene multi-proxy environmental reconstruction from lake Hakluytvatnet, Amsterdamøya Island, Svalbard (79.5°N). *Quaternary Science Reviews*. doi: 10.1016/j.quascirev.2017.02.017.

Grimm, E. C. (1987). CONISS: a FORTRAN 77 program for stratigraphically constrained cluster analysis by the method of incremental sum of squares. *Computers & geosciences*, 13 (1): 13-35.

Hadač, E. (1989). Notes on plant communities of Spitsbergen. *Folia Geobotanica et Phytotaxonomica*, 24 (2): 131-169.

Hofreiter, M., Serre, D., Poinar, H., Kuch, M. & Pääbo, S. (2001). Ancient DNA. *Nature Reviews*, 2.

Holmgren, S. U., Bigler, C., Ingólfsson, O. & Wolfe, A. P. (2010). The Holocene–Anthropocene transition in lakes of western Spitsbergen, Svalbard (Norwegian High Arctic): climate change and nitrogen deposition. *Journal of Paleolimnology*, 43 (2): 393-412.

Hongve, D. (1997). Cycling of iron, manganese, and phosphate in a meromictic lake. *Limnology and Oceanography*, 42 (4): 635-647.

Hyvärinen, H. (1970). Flandrian Pollen Diagrams from Svalbard. *Geografiska Annaler. Series A, Physical Geography*, 52 (3): 213-222.

IPCC. (2013). Summary for Policymakers. In Stocker, T. F., Qin, D., Plattner, G.-K., Tignor, M., Allen, S. K., Boschung, J., Nauels, A., Xia, Y., Bex, V. & Midgley, P. M. (eds). *Climate Change 2013: The Physical Science Basis. Contribution of Working Group I to the Fifth Assessment Report of the Intergovernmental Panel on Climate Change*. Cambridge, UK & New York, NY, USA.

Jari Oksanen, F. Guillaume Blanchet, Michael Friendly, Roeland Kindt, Pierre Legendre, Dan McGlinn, Peter R. Minchin, R. B. O'Hara, Gavin L. Simpson, Peter Solymos, M. Henry H. Stevens, Eduard Szoecs and Helene

Wagner (2017). vegan: Community Ecology Package. R package version 2.4-4. https://CRAN.R-project.org/package=vegan

Juggins, S. (2017) rioja: Analysis of Quaternary Science Data, R package version (0.9-15.1).(http://cran.r-project.org/package=rioja).

Jørgensen, T., Haile, J., Möller, P. E. R., Andreev, A., Boessenkool, S., Rasmussen, M., Kienast, F., Coissac, E., Taberlet, P., Brochmann, C., et al. (2012). A comparative study of ancient sedimentary DNA, pollen and macrofossils from permafrost sediments of northern Siberia reveals long-term vegetational stability. *Molecular Ecology*, 21 (8): 1989-2003. doi: 10.1111/j.1365-294X.2011.05287.x.

Kylander, M. E., Ampel, L., Wohlfarth, B. & Veres, D. (2011). High-resolution X-ray fluorescence core scanning analysis of Les Echets (France) sedimentary sequence: new insights from chemical proxies. *Journal of Quaternary Science*, 26 (1): 109-117. doi: 10.1002/jqs.1438.

Legendre, P. & Birks, H. J. B. (2012). From Classical to Canonical Ordination. In Birks, H. J. B., Lotter, A. F., Juggins, S. & Smol, J. P. (eds) *Tracking Environmental Change Using Lake Sediments: Data Handling and Numerical Techniques*, pp. 201-248. Dordrecht: Springer Netherlands.

Lid, J. & Lid, D. (2005). Norsk flora. 7 utgåve ved R. *Elven. Det Norske Samlaget, Oslo, Norway*.

Luoto, T. P., Ojala, A. E. K., Arppe, L., Brooks, S. J., Kurki, E., Oksman, M., Wooller, M. J. & Zajączkowski, M. (2017). Synchronized proxy-based temperature reconstructions reveal mid- to late Holocene climate oscillations in High Arctic Svalbard. *Journal of Quaternary Science*. doi: 10.1002/jqs.3001.

Löwemark, L., Chen, H. F., Yang, T. N., Kylander, M., Yu, E. F., Hsu, Y. W., Lee, T. Q., Song, S. R. & Jarvis, S. (2011). Normalizing XRF-scanner data: A cautionary note on the interpretation of high-resolution records from organic-rich lakes. *Journal of Asian Earth Sciences*, 40 (6): 1250-1256. doi: 10.1016/j.jseaes.2010.06.002.

Mangerud, J. & Svendsen, J. I. (2018). The Holocene Thermal Maximum around Svalbard, Arctic North Atlantic; molluscs show early and exceptional warmth. *Holocene*, 28 (1): 65-83. doi: 10.1177/0959683617715701.

Melles, M., Brigham-Grette, J., Minyuk, P. S., Nowaczyk, N. R., Wennrich, V., DeConto, R. M., Anderson, P. M., Andreev, A. A., Coletti, A. & Cook, T. L. (2012). 2.8 million years of Arctic climate change from Lake El'gygytgyn, NE Russia. *science*: 1222135.

Miller, G. H., Brigham-Grette, J., Alley, R. B., Anderson, L., Bauch, H. A., Douglas, M. S. V., Edwards, M. E., Elias, S. A., Finney, B. P., Fitzpatrick, J. J., et al. (2010). Temperature and precipitation history of the Arctic. *Quaternary Science Reviews*, 29 (15-16): 1679-1715. doi: 10.1016/j.quascirev.2010.03.001.

Monitoring, A. (2012). *Arctic Climate Issues 2011: Changes in Arctic Snow, Water, Ice and Permafrost. SWIPA 2011 Overview Report*: Arctic Monitoring and Assessment Programme (AMAP).

Nathan, R. (2006). Long-distance dispersal of plants. *Science*, 313 (5788): 786-8. doi: 10.1126/science.1124975.

Nathan, R., Schurr, F. M., Spiegel, O., Steinitz, O., Trakhtenbrot, A. & Tsoar, A. (2008). Mechanisms of long-distance seed dispersal. *Trends in Ecology & Evolution*, 23 (11): 638-47. doi: 10.1016/j.tree.2008.08.003.

Norwegian Polar Institute/U.S. Geological Survey Landsat (2010). *NP Basiskart Svalbard WMS.* [Web map service]. Updated 29.11.2017. Modified by Voldstad, L. H. Accessed 31.01.2018 from https://geodata.npolar.no/arcgis/services/Basisdata/NP_Basiskart_Svalbard_WMS/MapServer/WMSServer?request=GetCapabilities&service=WMS. *OGC WMS 1.3.0*.

Norwegian Polar Institute (2014a). Kartdata Svalbard 1:100 000 (S100 Kartdata) / Map Data [Data set]. Updated Sep. 2017. Norwegian Polar Institute. Accessed 31.01.2018 from https://doi.org/10.21334/npolar.2014.645336c7. *Shapefile.*

Norwegian Polar Institute (2014b). Terrengmodell Svalbard (S0 Terrengmodell) [Data set]. Updated 14.09.2017. Norwegian Polar Institute. Accessed 31.01.2018 from https://doi.org/10.21334/npolar.2014.dce53a47. *TIF*

Parducci, L., Bennett, K. D., Ficetola, G. F., Alsos, I. G., Suyama, Y., Wood, J. R. & Pedersen, M. W. (2017). Ancient plant DNA from lake sediments: Notes S1 Bioinformatic tools for metabarcoding datasets. *New Phytologist*, 214 (3).

Pedersen, M. W., Ginolhac, A., Orlando, L., Olsen, J., Andersen, K., Holm, J., Funder, S., Willerslev, E. & Kjær, K. H. (2013). A comparative study of ancient environmental DNA to pollen and macrofossils from lake sediments

reveals taxonomic overlap and additional plant taxa. *Quaternary Science Reviews*, 75: 161-168. doi: 10.1016/j.quascirev.2013.06.006.

Pedersen, M. W., Ruter, A., Schweger, C., Friebe, H., Staff, R. A., Kjeldsen, K. K., Mendoza, M. L., Beaudoin, A. B., Zutter, C., Larsen, N. K., et al. (2016). Postglacial viability and colonization in North America's ice-free corridor. *Nature*, 537 (7618): 45-49. doi: 10.1038/nature19085.

Reimer, P. J., Bard, E., Bayliss, A., Beck, J. W., Blackwell, P. G., Ramsey, C. B., Buck, C. E., Cheng, H., Edwards, R. L., Friedrich, M., et al. (2013). Intcal13 and Marine13 Radiocarbon Age Calibration Curves 0-50,000 Years Cal Bp. *Radiocarbon*, 55 (4): 1869-1887. doi: DOI 10.2458/azu_js_rc.55.16947.

Rothwell, G., Hoogakker, B., Thompson, J., Croudace, I. W. & Frenz, M. (2006). Turbidity emplacement on the southern Balearic Abyssal Plain (western Mediterranean Sea) during Marine Isotope Stages 1-3: an application of ITRAX XRF scanning of sediment cores to litostratigraphic analysis. In Rothwell, R. G. (ed.) Special Publications, vol. 267 *New Techniques in Sediment Core Analysis.* , pp. 79–98. London: Geological Society.

Rothwell, R. G. & Rack, F. R. (2006). *New techniques in sediment core analysis: an introduction*. Special Publications, vol. 267. London: Geological Society.

Rothwell, R. G. & Croudace, I. w. (2015). Twenty Years of XRF Core Scanning Marine Sediments: What Do Geochemical Proxies Tell Us? In Developments in Paleoenvironmental Research, *Micro-XRF Studies of Sediment Cores*, pp. 25-102.

Rønning, O. I. (1996). *The flora of Svalbard*.

Røthe, T. O., Bakke, J., Vasskog, K., Gjerde, M., D'Andrea, W. J. & Bradley, R. S. (2015). Arctic Holocene glacier fluctuations reconstructed from lake sediments at Mitrahalvøya, Spitsbergen. *Quaternary Science Reviews*, 109: 111-125. doi: 10.1016/j.quascirev.2014.11.017.

Salvigsen, O. & Høgvard, K. (2006). Glacial history, Holocene shoreline displacement and palaeoclimate based on radiocarbon ages in the area of Bockfjorden, north-western Spitsbergen, Svalbard. *Polar Research*, 25 (1): 15-24.

Sandgren, P. & Snowball, I. (2001). Application of mineral magnetic techniques to paleolimnology. In Last, W. M. & Smol, J. P. (eds) vol. 2 *Tracking Environmental Change Using Lake Sediments, Physical and Chemical Techniques*. Dordrecht, The Netherlands.: Kluwer Academic Publishers.

Schomacker, A., Brynjólfsson, S., Andreassen, J. M., Gudmundsdóttir, E. R., Olsen, J., Odgaard, B. V., Håkansson, L., Ingólfsson, Ó. & Larsen, N. K. (2016). The Drangajökull ice cap, northwest Iceland, persisted into the early-mid Holocene. *Quaternary Science Reviews*, 148: 68-84. doi: 10.1016/j.quascirev.2016.07.007.

Soininen, E. M., Gauthier, G., Bilodeau, F., Berteaux, D., Gielly, L., Taberlet, P., Gussarova, G., Bellemain, E., Hassel, K., Stenoien, H. K., et al. (2015). Highly overlapping winter diet in two sympatric lemming species revealed by DNA metabarcoding. *PLoS One*, 10 (1): e0115335. doi: 10.1371/journal.pone.0115335.

Sønstebø, J. H., Gielly, L., Brysting, A. K., Elven, R., Edwards, M., Haile, J., Willerslev, E., Coissac, E., Rioux, D., Sannier, J., et al. (2010). Using next-generation sequencing for molecular reconstruction of past Arctic vegetation and climate. *Mol Ecol Resour*, 10 (6): 1009-18. doi: 10.1111/j.1755-0998.2010.02855.x.

Taberlet, P., Coissac, E., Pompanon, F., Gielly, L., Miquel, C., Valentini, A., Vermat, T., Corthier, G., Brochmann, C. & Willerslev, E. (2007). Power and limitations of the chloroplast trnL (UAA) intron for plant DNA barcoding. *Nucleic Acids Res*, 35 (3): e14. doi: 10.1093/nar/gkl938.

Team, R. C. (2017). *R: A language and environment for statistical computing.* Vienna, Austria.: R Foundation for Statistical Computing.

Thompson, R., Battarbee, R. W., Osullivan, P. E. & Oldfield, F. (1975). Magnetic-Susceptibility of Lake Sediments. *Limnology and Oceanography*, 20 (5): 687-698. doi: DOI 10.4319/lo.1975.20.5.0687.

van der Bilt, W. G. M., Bakke, J., Vasskog, K., D'Andrea, W. J., Bradley, R. S. & Ólafsdóttir, S. (2015). Reconstruction of glacier variability from lake sediments reveals dynamic Holocene climate in Svalbard. *Quaternary Science Reviews*, 126: 201-218. doi: 10.1016/j.quascirev.2015.09.003.

Vasil'chuk, A. (2005). Taphonomic features of Arctic pollen. *Biology Bulletin*, 32 (2): 196-206.

Willerslev, E., Davison, J., Moora, M., Zobel, M., Coissac, E., Edwards, M. E., Lorenzen, E. D., Vestergard, M., Gussarova, G., Haile, J., et al. (2014). Fifty thousand years of Arctic vegetation and megafaunal diet. *Nature*, 506 (7486): 47-51. doi: 10.1038/nature12921.

Wilson, I. G. (1997). Inhibition and facilitation of nucleic acid amplification. *Applied and environmental microbiology*, 63 (10): 3741.

QGIS Development Team (2016). QGIS Geographic Information System. Open Source Geospatial Foundation Project. http://qgis.osgeo.org

Appendix

Table B: Settings for age-depth modelling of piston and surface core with Bacon 2.2.

Function	Piston core setting	Surface core setting
#d.min	8	2.5
#d.max	185.5	27
#thick	5	2
#d.by	1	1
#depths.file	1	1
#slump	NA	NA
#acc.mean	50	0.1
#acc.shape	1.5	1.5
#mem.mean	0.7	0.7
#mem.strength	4	4
#hiatus.depths	NA	NA
#hiatus.mean	1000	1000
#hiatus.shape	1	1
#BCAD	0	0
#cc	1	1
0 #postbomb	0	0
#cc1	IntCal13	IntCal13
#cc2	Marine13	Marine13
#cc3	SHCal13	SHCal13
#cc4	ConstCal	ConstCal
#unit	cm	cm
#normal	0	0
#t.a	3	3
#t.b	4	4
#d.R	0	0
#d.STD	0	0
#prob	0.95	0.95

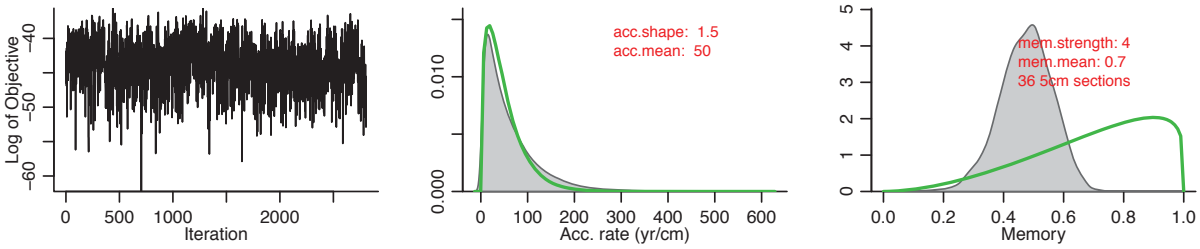

Figure B: Output graphs from *Bacon*: (left) stability of the model in terms of MCMC iterations; (middle) prior (green line) and posterior (filled grey) distribution of accumulation mean; and (right) prior (green line) and posterior (filled grey) distribution of memory properties. The relatively stationary and unstructured adjacent iterations indicate a good model-run.

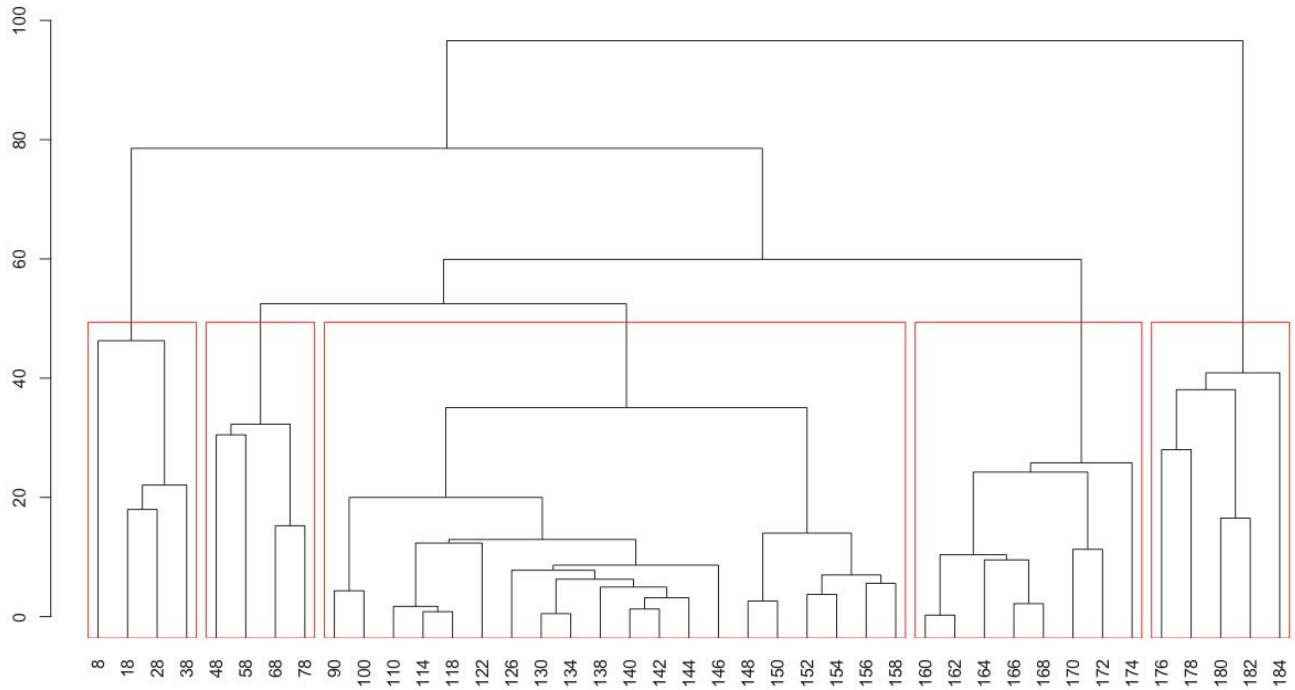

Figure B: Dendrogram from constrained hierarchical clustering of scaled and centred ITRAX-data corresponding to sample depths for *sed*aDNA samples.

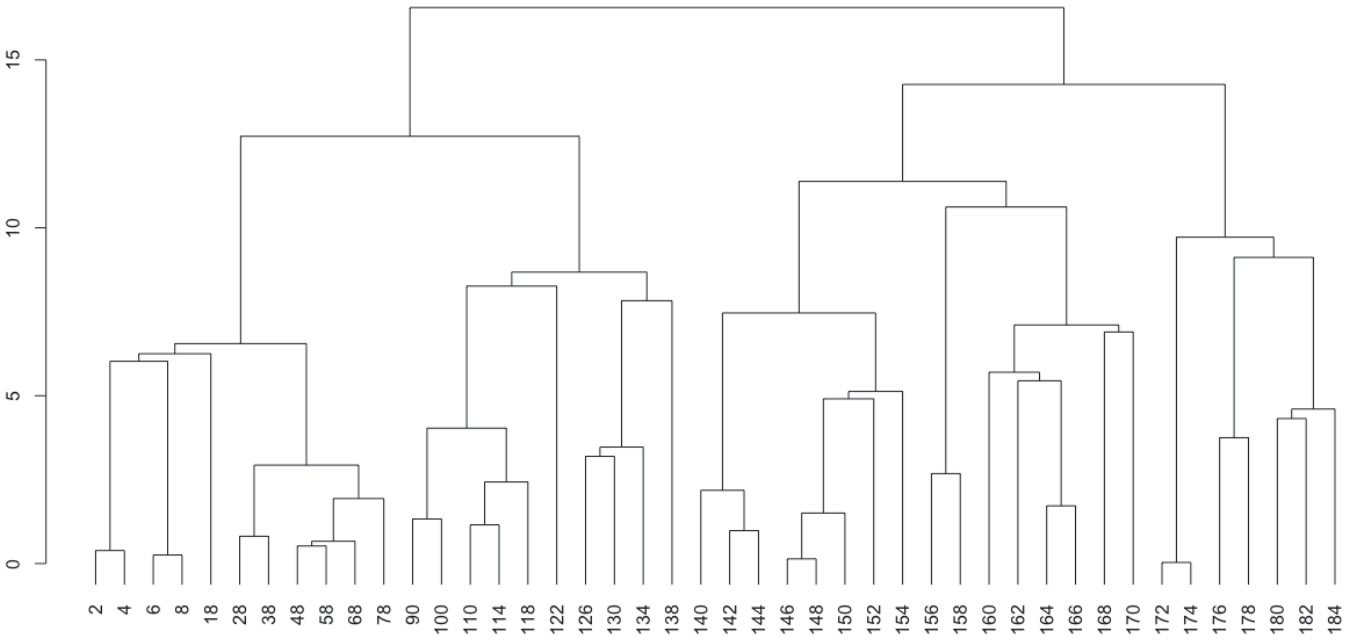

Figure C: Dendrogram from constrained hierarchical clustering of PCR repeats per sample from aDNA data. The clusters are based on sample depths (cm; x-axis) and constrained by sample order. The branch-split indicates the distance (y-axis) between the clusters at the point they were separated in the cluster analysis.

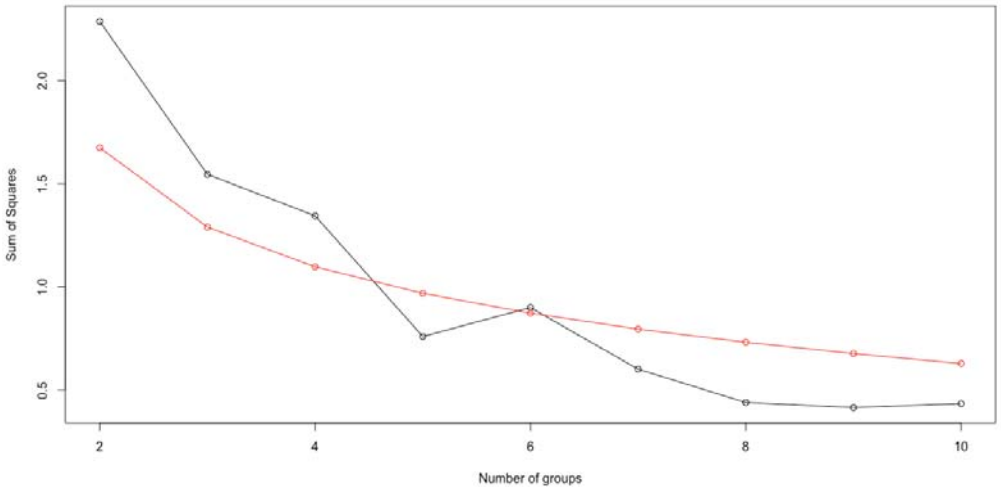

Figure D: Graphical display of broken stick model with the observed reduction in within-group sums of squares (y-axis) plotted in black and the broken stick distribution in red. Five significant stratigraphic zones are interpreted by comparing the dispersion of the constrained hierarchical classification to the dispersion obtained from a broken stick model (from the point on the x-axis where the reduction in variance exceeds the proportion expected from the broken stick model). Because this particular zone accounts for more variance than would have been expected if the dataset consisted of randomly arranged samples, it can be considered significant (Bennett, 1996).

Table B: Summary of number of PCR repeats from aDNA taxa present in the detected stratigraphic zones Z1-Z5.

Zone	**Z1**	**Z2**	**Z3**	**Z4**	**Z5**
Sample Depth	185-172 cm	171-156 cm	155-140 cm	139-90 cm	79-2 cm
Cal. age BP	11760-10150	9935-8460	8240-6750	6500-3750	3200-160
Calamagrostis neglecta/purpurascens	0	0	0	0	6
Arnica angustifolia	0	2	0	1	1
Asteraceae	2	0	0	0	12
Bistorta vivipara	2	0	33	31	74
Brassicaceae	0	0	2	0	0
Braya glabella	0	0	0	0	17
Cardamine bellidifolia	0	0	0	0	14
Carex sp.	2	0	4	1	48
Cassiope tetragona	0	0	0	12	90
Cerastium	1	0	0	1	13
Cochlearia groenlandica	1	0	0	0	6
Draba	4	1	0	2	30
Dryas octopetala	1	0	0	46	72
Empetrum nigrum	0	3	12	15	1
Equisetum arvense	12	4	4	2	4
Equisetum variegatum/scirpoides	0	1	4	4	4
Festuca sp.	0	2	0	2	58
Huperzia arctica	0	0	0	3	0
Juncus biglumis	2	0	0	0	19
Juniperus	0	0	0	0	2

Luzula sp.	0	0	0	0	34
Oxyria digyna	0	2	2	10	58
Papaver sp.	11	0	0	0	24
Pedicularis	0	0	0	4	14
Poeae	1	0	0	0	15
Poinae	0	0	0	0	19
Cystopteris fragilis	8	0	0	1	0
Potentilla sp.	6	0	2	0	74
Ranunculus hyperboreus	3	0	0	0	0
Ranunculus sceleratus	6	0	0	0	0
Minuartia rubella	1	0	0	0	4
Sagina nivalis/caespitosa	1	0	0	0	8
Saliceae	0	0	19	44	76
Saxifraga cer/riv/hyp	6	0	0	3	76
Saxifraga sp.	26	7	7	15	70
Saxifraga cespitosa	4	1	1	1	3
Saxifraga oppositifolia	18	6	6	21	74
Micranthes hier/tenu/niv	2	0	2	2	31
Silene acaulis	0	0	2	3	12
Stellaria longipes	0	0	0	0	17
Number of vascular taxa	**22**	**10**	**14**	**22**	**35**
% vascular taxa	**55,0**	**25,0**	**35,0**	**55,0**	**87,5**
Andreaea nivalis	0	0	0	0	2
Timmia norvegica/austriaca	0	0	1	0	8
Bryum pallens	1	0	0	0	8
Polytrichaceae	6	0	0	12	25
Pottiaceae	2	0	0	0	0
Bartramiaceae	0	0	0	0	9
Bryum	4	4	0	5	30
Bryaceae	1	0	1	0	14
Dicranaceae	0	0	0	0	6
Distichium capillaceum/inclinatum	2	1	0	0	9
Hypnales	41	1	10	3	16
Encalypta rhaptocarpa/streptocarpa	1	0	0	0	4
Number of bryophyte taxa	**8**	**3**	**3**	**3**	**11**
% bryophyte taxa	**66,7**	**25,0**	**25,0**	**25,0**	**91,7**
Closterium baillyanum	0	10	0	1	21
Cosmarium botrytis	1	8	2	9	51
Nannochloropsis granulata	3	36	49	4	2
Neglectella solitaria	0	5	0	0	0
Staurastrum punctulatum	0	0	0	0	3
Total algae taxa	**2**	**4**	**2**	**3**	**4**
% algae taxa	**40**	**80**	**40**	**60**	**80**
Number of total taxa	**32**	**17**	**19**	**28**	**50**
% taxa overall	**47,8**	**25,4**	**28,4**	**41,8**	**74,6**

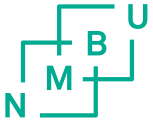

Norges miljø- og biovitenskapelige universitet
Noregs miljø- og biovitskapelege universitet
Norwegian University of Life Sciences

Postboks 5003
NO-1432 Ås
Norway